

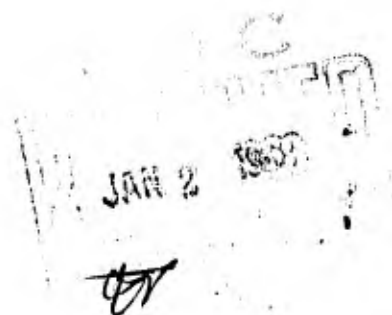
AD 664236



PWA FR-2631A
13 NOVEMBER 1967

DESIGN AND EVALUATION OF A HIGH TEMPERATURE RADIAL TURBINE

QUARTERLY TECHNICAL PROGRESS REPORT NO. 1
For The Period 18 July Through 31 October 1967



This report has been approved
for release and order its
distribution is unlimited.

Prepared Under *new*
Contract DAAJ02-68-C-0003
For
U. S. Army Aviation Materiel Laboratories
Ft. Eustis, Virginia

Pratt & Whitney Aircraft
FLORIDA RESEARCH AND DEVELOPMENT CENTER

DIVISION OF UNITED AIRCRAFT CORPORATION
**U
A.**

Reproduced by the
CLEARINGHOUSE
for General Scientific & Technical
Information Springfield, Va. 22151

UNCLASSIFIED

AD 664 236

DESIGN AND EVALUATION OF A HIGH TEMPERATURE
RADIAL TURBINE

Pratt and Whitney Aircraft
West Palm Beach, Florida

November 1967

Processed for . . .

DEFENSE DOCUMENTATION CENTER
DEFENSE SUPPLY AGENCY



U. S. DEPARTMENT OF COMMERCE / NATIONAL BUREAU OF STANDARDS / INSTITUTE FOR APPLIED TECHNOLOGY

UNCLASSIFIED

UNCLASSIFIED

1. Distribution of this document is unlimited.
2. This document is subject to special export controls and each transmittal to foreign governments or foreign nationals may be made only with prior approval of US Army Aviation Materiel Laboratories, Fort Eustis, Virginia 23604.
3. In addition to security requirements which must be met, this document is subject to special export controls and each transmittal to foreign governments or foreign nationals may be made only with prior approval of USAAVLABS, Fort Eustis, Virginia 23604.
4. Each transmittal of this document outside the agencies of the US Government must have prior approval of US Army Aviation Materiel Laboratories, Fort Eustis, Virginia 23604.
5. In addition to security requirements which apply to this document and must be met, each transmittal outside the agencies of the US Government must have prior approval of US Army Aviation Materiel Laboratories, Fort Eustis, Virginia 23604.
6. Each transmittal of this document outside the Department of Defense must have prior approval of US Army Aviation Materiel Laboratories, Fort Eustis, Virginia 23604.
7. In addition to security requirements which apply to this document and must be met, each transmittal outside the Department of Defense must have prior approval of US Army Aviation Materiel Laboratories, Fort Eustis, Virginia 23604.
8. This document may be further distributed by any holder only with specific prior approval of US Army Aviation Materiel Laboratories, Fort Eustis, Virginia 23604.
9. In addition to security requirements which apply to this document and must be met, it may be further distributed by the holder only with specific prior approval of US Army Aviation Materiel Laboratories, Fort Eustis, Virginia 23604.

DISCLAIMER

10. The findings in this report are not to be construed as an official Department of the Army position unless so designated by other authorized documents.

11. When Government drawings, specifications, or other data are used for any purpose other than in connection with a definitely related Government procurement operation, the United States Government thereby incurs no responsibility nor any obligation whatsoever; and the fact that the Government may have formulated, furnished, or in any way supplied the said drawings, specifications, or other data is not to be regarded by implication or otherwise as

... of the ...
... of the ...
... of the ...

12. This report shall be destroyed as soon as possible after the final endorsement of approval or disapproval of the commanding officer of the unit.

DISPOSITION OF THIS REPORT

13. Destroy this report when no longer needed. Do not return it to originator.

14. When this report is no longer needed, Department of the Army organizations will destroy it in accordance with the procedures given in AR 380-9.

U.S. Army Aviation Materiel Laboratories
Fort Belvoir, Va. 23604

This Quarterly Report is an Interim Engineering Report covering work performed under Contract DAAJ02-68-C-0003 from 18 July 1967 through 31 October 1967. It is published for information only and does not necessarily represent the recommendations, conclusions or approval of the Army.

Edward T. Johnson
USA AVLABS Project Engineer

PWA FR-2631A
13 NOVEMBER 1967

DESIGN AND EVALUATION
OF A
HIGH TEMPERATURE RADIAL TURBINE

QUARTERLY TECHNICAL PROGRESS REPORT NO. 1
For The Period 18 July Through 31 October 1967



Prepared by:

G. S. Calvert
G. S. Calvert
Program Manager

Approved by:

M. T. Schilling
M. T. Schilling
Project Engineer

Prepared Under
Contract DAAJ02-68-C-0003
For
U. S. Army Aviation Materiel Laboratories
Ft. Eustis, Virginia

Pratt & Whitney Aircraft DIVISION OF UNITED AIRCRAFT CORPORATION
FLORIDA RESEARCH AND DEVELOPMENT CENTER



CONTENTS

SECTION		PAGE
	ILLUSTRATIONS	iii
I	INTRODUCTION	1
II	TECHNICAL DISCUSSION	2
	A. Task 1 - Control Layout.	2
	B. Task 2 - Aerodynamic Design.	2
	C. Task 3 - Structural and Mechanical Design.	7
	D. Task 4 - Heat Transfer Analysis.	9
	E. Task 5 - Fabrication Study	12
	F. Task 6 - Cold Flow Tests	13
III	WORK PLANNED FOR NEXT REPORT PERIOD.	14

ILLUSTRATIONS

FIGURE		PAGE
1	Control Layout High Temperature Radial Turbine Test Rig.	15
2	Radial Turbine Rotor Terminology.	16
3	Radial Turbine Nozzle Terminology	17
4	Calculated Channel Velocity Distribution is Identical for All Cold Flow Nozzles	18
5	15-Vane Nozzle Streamline Pattern	19
6	20-Vane Nozzle Streamline Pattern	20
7	25-Vane Nozzle Streamline Pattern	21
8	25-Modified-Vane Streamline Pattern (1)	22
9	25-Modified-Vane Streamline Pattern (2)	23
10	15-Vane Nozzle.	24
11	20-Vane Nozzle.	25
12	25-Vane Nozzle.	26
13	Radial Turbine Rotor.	27
14	Water Visualization Rig	28
15	Cooled Turbine Preliminary Design - 75-Degree Nozzle Angle.	29
16	Cooled Turbine Preliminary Design - 70-Degree Nozzle Angle.	30
17	Cooled Turbine Preliminary Design - 80-Degree Nozzle Angle.	31
18	Effects of Nozzle and Rotor Losses on Turbine Efficiency.	32
19	Cooled Turbine Rotor: First-Iteration Blade Thickness Distribution.	33
20	First-Iteration Cooled Turbine Design	34
21	Second Iteration Design	35
22	First-Iteration Nozzle Heat Transfer Design	36
23	Second-Iteration Nozzle Heat Transfer Design: Nozzle Uses Shroud Air.	37
24	First-Iteration Rotor Heat Transfer Design Shows Reduced Pedestal Density.	38
25	Pressure Surface Temperature Distribution	39
26	Suction Surface Temperature Distribution.	40

ILLUSTRATIONS (Continued)

FIGURE		PAGE
27	Hot Turbine Part Load Efficiency Estimated From Results of Previous Tests.	41
28	Hot Turbine Swallowing Capacity Estimated From Results of Previous Tests.	42

SECTION I
INTRODUCTION

Radial turbines offer greater stage work capacity than axial turbines. If this advantage can be coupled with a capability of accommodating high turbine inlet temperatures, radial turbines will permit appreciable simplification of small gas turbine engines for use in future Army vehicles. The objective of this contract is to develop a technology for high temperature radial turbines to a level that will permit a potential small-engine manufacturer to make a choice between the radial and axial turbine.

A two-year, two-phase program is being conducted involving the design and testing of a cooled, single-stage, radial-inflow turbine with the following design conditions: 2300°F turbine inlet temperature, total-to-total aerodynamic efficiency of 87.5%, gas flow of 5 lb/sec, and stage work parameter ($-\Delta H/\theta$) of 42.5 Btu/lb. The first phase of the program involves a preliminary design of the cooled radial turbine, including development of cold flow data to permit design optimization. In the second phase, the design will be finalized, and the cooled radial turbine will be fabricated and tested. The report headings used herein are consistent with the contractual tasks. Only Phase I tasks are included, as Phase II effort is not scheduled until the twelfth month of the contract.

During this quarter, a seven-week UAW-CIO strike occurred at UACL. Union members returned to work on 25 September 1967. Because of the strike, two items in the program have been delayed; the in-house fabrication of the water rig was delayed for about seven weeks, and the detail design of the cold flow nozzles was delayed for about two weeks. Only the cold flow nozzles should affect the overall period of performance. Every effort will be made to minimize the time lost to the program.

SECTION II
TECHNICAL DISCUSSION

A. TASK 1 - CONTROL LAYOUT

First Version of Control Layout Designated

The layout that was presented as a preliminary concept in proposal PWA FP 67-39 has been designated as the first version of the Control Layout, and it is included in this report as figure 1*. Changes to this layout will be incorporated whenever they are indicated by any of the current studies or cold flow tests. Since the aerodynamic/structural/heat transfer analyses are iterating on a preliminary design, no changes have been made to the Control Layout during this report period.

B. TASK 2 - AERODYNAMIC DESIGN

Radial Turbine Terminology Defined

Figures 2 and 3 are presented to clarify radial turbine terminology.

Cold Flow Nozzle Aerodynamics Defined

The aerodynamic design for the three new cold-flow nozzle sections was completed in August. These new nozzle sections will have 15, 20, and 25 vanes with 0.025-in. trailing edge radii.

The three new nozzle sections were designed as members of a consistent family of nozzles with the following parameters held constant:

1. Vane span (i.e., the axial dimension for a radial vane)
2. Radius to trailing edge center
3. Total throat area
4. Trailing edge thickness
5. Angle between inlet stagnation streamline and line tangent to suction surface at suction surface intersection with leading edge radius.

The following parameters were varied (by necessity) for the new designs:

1. Wetted wall area per nozzle passage
2. Throat aspect ratio, defined as the span divided by the throat dimension
3. Trailing edge wedge angle.

*Figures follow text

The resulting nozzle designs have identical calculated channel velocity distributions, which are shown in figure 4. Note that in this figure the flow is accelerating on both walls with an increased acceleration on the suction surface near the throat. In nozzle design practice it is not uncommon to have local diffusion at the throat on the suction surface, although the flow is accelerating overall. The design shown in figure 4 is desirable to reduce the boundary layer thickness and thereby improve nozzle efficiency.

Nozzle Leading Edge Orientation Prevents Separation

Figures 5, 6, and 7 present calculated potential flow streamlines for the three new nozzle sections. These figures show that the three sections were designed to have similar leading edge geometries, i.e., the leading edge is aligned with the anticipated incident flow direction.

To illustrate the importance of correct leading edge orientation, potential flow streamlines have been calculated for the basic 25-vane nozzle with a progressively reduced chord. If vane chord were reduced by simply cutting back on the leading edge, leaving the rest of the vane untouched, the streamline pattern would look like that shown in figure 8. Part of the flow in passing around the leading edge would feel a rather high local curvature that would produce a high local velocity. This high velocity at the leading edge cannot be maintained, since the suction surface curvature decreases towards the throat, i.e., local diffusion takes place. When this diffusion becomes sufficiently high, a real gas would separate from the suction surface. While the flow would probably reattach before the throat due to the high overall acceleration in the channel, total pressure loss would be increased and flow would become unsteady. Figure 9 shows the leading edge cut back even further. Now the circulation imposed by the vane moves the leading edge stagnation streamline farther away from the leading edge and the flow next to the suction surface would certainly separate. While this vane design might be suitable for a turbine having a nonradial inlet flow direction, it is clearly not adequate for the present design.

Cold Flow Nozzles and Rotors Being Fabricated

The detail designs of the cold-flow nozzles are presented in figures 10, 11, and 12. The UAW strike at UACL delayed the completion of these designs, but the 15-vane section was released for manufacture in September, and the 20- and 25-vane sections were released in October.

The new cold-flow rotors, having 10 and 12 blades, were designed and released for manufacture in August. As indicated by the part number table in figure 13, the new rotors are essentially the same as the existing 14-blade rotor, except for the reduced number of blades.

Water Flow Rig Designed and Fabricated

The design of the water visualization rig has been completed, and the rig has been fabricated. A layout of the complete rig is presented in figure 14.

This rig incorporates a rotating mirror optical system and a high-speed movie camera to record the movement of water flow relative to a turbine blade. A transparent viewing port will permit the photographic system to follow a single rotor blade through approximately 1/4 of a revolution.

The optical system follows the principle shown in the proposal. A fixed camera is aimed at a mirror located on the centerline and above the turbine wheel. This mirror rotates at 1/2 turbine speed, and the effective line of sight thus rotates at turbine speed along a single radial line on the turbine rotor. At the rim, another mirror mounted on this radial line (i.e., rotating with the turbine) deflects the line of sight down through the blades, so the camera sees an image in which the rotor blades are fixed and the nozzle vanes rotate. During the period in which the central mirror is at a usable angle, the view is the same as that of a camera mounted approximately 4 ft above the turbine rim, looking down through the blades and rotating with the turbine wheel. Surface-aluminized mirrors are used to eliminate multiple secondary images.

By the use of a system in which the final viewing device is fixed, there are no restrictions on camera type, other than the minimum distance requirement of approximately 4 ft. The image could in fact be viewed by eye, although the intermittent presentation would make interpretation difficult.

The camera that will be used with this rig is a Wollensak WF4 16-mm Fastax that is capable of speeds up to 9000 frames per second. Usable speed will probably be limited by light intensity (from a 1 kw lamp) to about 1000 frames/second. At normal projection speed of 16 frames-per-second this gives a time magnification of more than 60. Assuming 12 blades and 30 rpm, a rotor blade channel passes a fixed point in about 1/6 second, and this event will thus be expanded to 10 seconds on projection.

Water streamlines, both for the primary (driving) flow and the secondary (cooling) flow, will be made visible through the generation of tiny hydrogen bubbles. These hydrogen bubbles will be generated by electrolysis of the water. Electrodes will be located both in the nozzles (for primary flow streamlines) and at the rotor leading edge (for secondary flow streamlines). Only one set of electrodes will be energized at a time to avoid confusion between primary and secondary streams. During our pre-proposal studies, dyed water was considered for the coolant flow, but this system was discarded in favor of the simpler and more reliable hydrogen bubble design. The hydrogen system also has the capability of producing time-marked flow patterns to indicate fluid velocities. This is possible because modulation of the electric current producing the electrolytic action produces a similarly modulated flow of hydrogen bubbles.

Hot Turbine Velocity Triangles Finalized

The mean-line design of the cooled turbine was finalized in September. A meridional view of the turbine rotor, the inlet and exhaust velocity triangles, and other design data are presented in figure 15.

The rotor tip absolute flow angle, as shown in figure 15, is 75 deg. This value was chosen as a compromise between a lower flow angle (desirable for low rotor blade centrifugal stresses) and a higher flow angle (desirable for high flow acceleration within the rotor). In the proposal, the preliminary nozzle angle was shown as 70 deg and the nozzle span was 0.250 in. for a flow rate of 5 lb/sec. The new flow angle of 75 deg will require a span increase to 0.339 in. to pass the design flow of 5 lb/sec. Figures 16 and 17 show how the turbine profile and velocity triangles are affected by changing the nozzle angle to 70 and 80 deg, respectively.

A relative flow angle of 15 deg at the rotor inlet is shown on figure 15. This value was chosen as a compromise between a large relative angle (corresponding to a reduced rotor diameter) that would result in lower centrifugal stresses, and a lower or slightly negative relative flow angle (corresponding to an increased rotor diameter) that would minimize aerodynamic losses.

The preliminary number of blades for the cooled rotor has been chosen at 12. A small number of blades is desirable to reduce hub stresses and the rotor cooling air required. Cold flow tests that will be conducted later in Phase I (Task 6) will shed additional light on this choice of blade number.

The rotor exit area and the absolute flow angle (zero) shown in the velocity triangles of figure 15 were chosen so that the duct losses downstream of the turbine would be small in an engine application.

Figure 18 shows the calculated effect on turbine total-total efficiency caused by changes in nozzle energy coefficient and rotor efficiency. Note that an improvement in rotor efficiency of 1% produces a 0.46% improvement in turbine efficiency. A change of 0.01 in the nozzle loss coefficient ($1-\phi_N^2$) produces a 0.38% change in turbine efficiency. Thus the turbine efficiency is more sensitive to the rotor efficiency than to nozzle efficiency (i.e., ϕ_N^2).

Detail Design of Hot Nozzle and Rotor in Progress

At present, aerodynamic design of the nozzle consists of minor shape modifications of the basic 20-vane scheme, and the calculation of primary flow temperatures, pressures, and velocities as required for heat transfer design. The final aerodynamic design of the cooled nozzle hinges on the total quantity of cooling air exhausted through the nozzles and on the desired location for cooling air ejection, and therefore constitutes part of an iterative aerodynamic/heat transfer design cycle. Work on the second iteration is now underway (see Paragraph D, Task 4). Cold flow tests (Task 6) will indicate if the preliminary choice of 20 vanes (indicated in figure 15) is optimum.

Aerodynamic design of the rotor, based on the 12-blade scheme and the first-iteration blade thickness distribution, is currently in progress. Convergence problems associated with the chosen rotor geometry have so far prevented the completion of the flow analysis program, but preliminary results are sufficiently conclusive that analysis of a somewhat shortened rotor with modified shroud and hub curvatures was initiated, still using the first-iteration blade thickness distribution. The goal is to arrive at the shortest rotor in which the flow remains attached: such a design has the smallest practical wetted area (hence lowest friction losses) and the smallest rotor mass.

C. TASK 3 - STRUCTURAL AND MECHANICAL DESIGN

Dual Analyses Being Used For Blade Thickness Distribution

We have been using two approaches to determine the optimum blade thickness distribution for the cooled turbine: a graphical solution, and a new analytical solution.

The graphical solution being used is a refined version of a routine that was used in the design of the existing 14-blade rotor. In the past, this method has produced rotors with satisfactory aerodynamic shapes and an acceptable, though conservative, structural design (e.g., the existing 14-blade design). The graphical solution has been used for a preliminary assessment of the high temperature turbine. However, this method does not

1. Accurately assess the effect of cooling passages and nonload-carrying structures such as pedestals
2. Take full advantage of the increased manufacturing flexibility inherent with castings.

The new analytical stress program is intended to reduce the shortcomings of the graphical solution in these two areas.

Several test calculations have been made using both types of analysis. The simpler interpolation routine, using two reference sections, has proved more suitable for the current phase of the investigation.

Initial Rotor Blade Thickness Distribution Defined - Stress Analysis in Progress

The first-iteration blade thickness distribution for the cooled rotor was issued in September as a basis for further aerodynamic, thermal, and stress analysis. This thickness distribution, which is shown in figure 19, can accommodate the presently proposed cooling cavity. This thickness distribution will be optimized in the design iteration.

The first results from the stress analysis of the complete rotor indicates acceptable stress levels in the hub. The blade cannot be adequately represented to be analyzed in the desired detail, but so far the general stress level from the centrifugal load is as intended. Further blade analysis is continuing with a finer grid. This should assist the thickness distribution optimization.

Initial Mechanical Design Completed in September

During September, a stress analysis of the shroud indicated high stresses near the preliminary location of the junction between the front shroud and nozzle platform, marked "A" on figure 20. This junction was modified to improve this condition. The junction was relocated downstream from A and cooling air was introduced midway up the shroud at B. The cooling air then flowed radially outward along the outside of the shroud and the nozzle casting, entered the cored passages in the nozzle vanes, and was finally ejected near the nozzle trailing edge.

The backplate cooling air in this design was introduced through the nozzle support member and flowed radially inward to a series of holes in the heatshield adjacent to the backplate. The air then flowed radially outward between the heatshield and the backplate, through the cylindrical nozzle support member, through the outside surface of the nozzle casting, and finally entered the cored passage in the nozzle vane. This cooling air also exhausted near the nozzle trailing edge.

Second-Iteration Mechanical Design Completed in October

As a result of the initial heat transfer iteration (see Paragraph D, Task 4 - Heat Transfer Analysis), the initial mechanical design was modified during October. The revised configuration is shown in figure 21.

In this design the nozzle leading edge is cooled by the injection of air from the rear shroud into the vane cavity via a small standpipe welded into the vane nozzle casting. This small standpipe carries a series of small holes that direct the cooling air directly onto the inner surface of the leading edge of the nozzle vane. This air then passes around the outside of the standpipe and exhausts through a slot adjacent to the trailing edge as in the previous design. From a fabrication standpoint, this approach to cooling the nozzle vane facilitates production of the nozzle casting because the core of the vane is now open on one side. This permits more accuracy in positional control of the ceramic core used in the production of the hollow nozzle vane.

Cooling air from the front shroud is directed to the mid-chord region of the nozzle vanes, where it mixes with the air from the impingement tube. The combined airstream then exhausts near the vane trailing edge.

The cooling air for both the front and back shrouds in the second-iteration design is taken from a zone ahead of the combustion chamber. This change from the first-iteration design is desirable to reduce the temperature of the cooling air entering the shrouds.

D. TASK 4 - HEAT TRANSFER ANALYSIS

Initial Nozzle Design Reduces Complexity

The initial heat transfer design of the high temperature nozzles was completed during August and is shown in figure 22. This design is the first of several iterations that will be performed to obtain the best compromise between the sometimes conflicting requirements of optimum mechanical and aerodynamic designs. This heat transfer analysis resulted in a simpler design than that shown in our proposal: the number of pedestal rows was reduced from seven (in the proposal) to three.

The material that is being used for the nozzle analysis is the cobalt-base alloy WI52 (PWA 653), which was selected instead of the nickel-base alloy IN100 (PWA 658) to take advantage of WI52's higher melting temperature.

Shroud Cooling Requirements Determined

As part of the initial heat transfer analysis, the cooling air required for the front and rear shrouds was calculated. This analysis showed that 3% airflow would be required for each, or a total of 6% airflow would be required for both shrouds. Since there is appreciable pressure loss across the shrouds, it is not feasible to exhaust the shroud cooling air to the high pressure region ahead of the nozzle vanes. A more logical location for the shroud cooling air exhaust is near the vane trailing edge where the static pressure is reduced. When this flow path is chosen, the shroud coolant can also be used to cool the nozzle vane, without additional nozzle coolant per se. However, this flow path would increase the temperature of the cooling air entering the vanes. Since it is desirable to obtain the cooling air from the coolest possible location, the shroud/vane cooling air in the second-iteration design bypasses the combustion chamber and is taken directly from the compressor discharge (see figure 21 and Paragraph C, Task 3 - Structural and Mechanical Design).

Second-Iteration Nozzle Design Completed

The second nozzle design, evolved during October, is presented in figure 23. This design differs from the first design in two respects: an impingement tube is used, and the trailing edge pedestals have been removed.

The impingement tube is used instead of the drilled holes shown on previous drawings for two reasons: the vane span has increased from 0.250 to 0.339 in. and the inlet temperature of the vane coolant has increased from 875°F in the preliminary design to 1050°F with the new coolant gas path. The increased span reduces the effectiveness of the former design because it requires a longer distance between impingement streams and possibly a less-effective impingement angle. The higher coolant temperature reduces the heat transfer capacity of the cooling air, and makes the more efficient normal impingement angle desirable.

The pedestals in the trailing edge region are removed in the second design because the higher airflow through the vanes does not require increased turbulence in this region.

Trailing Edge Thickness Now Determined By Heat Conduction

In the current nozzle design, the 6% airflow exhausting at the vane trailing edge is more than the 1.5% required to cool the airfoil alone, and therefore the tradeoff between vane coolant and trailing edge thickness as shown in our proposal is no longer pertinent to this configuration. The trailing edge thickness is then determined by the larger value of either the minimum fabricable thickness, or the minimum thickness required to conduct the heat from the vane to the sidewalls. According to the casting vendors contacted during the Fabrication Study, the minimum thickness for a casting is 0.020-0.025 in. Results of the heat transfer analysis show that a minimum trailing edge thickness of 0.040 in. is required to maintain acceptable vane metal temperatures through conduction to the sidewalls. This value is therefore shown on figure 23 as the trailing edge thickness.

First Heat Transfer Analysis of Rotor Completed

A detailed heat transfer analysis of the rotor was completed during October. The resultant cooling passage, shown in figure 24, has a reduced pedestal density. This configuration was analyzed for 3% cooling air entering the rotor at 860°F. Figures 25 and 26 show the steady-state metal temperatures on the pressure and suction sides, respectively. These temperatures will be used as the basis for further analysis of rotor stress.

In addition to the cooling configuration shown in figure 24, an alternative design is being considered. In this design, the rotor tip would be closed and the cooling air would be forced to flow out to the tip and then radially inward to the star-exducer transition area where it would be discharged into the main stream.

E. TASK 5 - FABRICATION STUDY

Three Casting Vendors to Provide Nozzle and Rotor Specimens

It has been concluded that the fabrication study outlined in our proposal was satisfactory insofar as the nozzles were concerned, but that a more informative rotor study is feasible. Instead of casting a simple specimen design like that shown in our proposal, a full-size radial turbine rotor cast in IN100 (PWA 658) would permit a more realistic metallurgical evaluation. Three investment casting vendors were visited and invited to produce sample castings as follows:

1. One typical segment of a WI52 (PWA 653) nozzle section having cooled vanes
2. Two IN100 radial turbine rotors with hollow blades in the star and curved blades in the exducer
3. One IN100 radial turbine rotor with hollow blades in the star but with straight blades in the exducer.

These rotors will be used to obtain metallurgical data from selected areas of the rotor.

Rotor Properties to be Determined by Structural Testing

Structural tests will be conducted in three areas of the rotor: in the hub, in the hub/blade interface, and in the blades. These tests will consist of two types: elevated-temperature tensile, and elevated-temperature creep-rupture. The tensile tests will be the conventional type, but conducted at an elevated temperature approximating that which will be experienced by the rotor during hot tests. The creep-rupture test will be essentially a creep test that is extended to failure, and will yield the information usually obtained from individual creep and stress-rupture tests. They also will be conducted at temperatures predicted for the cooled rotor.

A tentative test plan has been formulated to evaluate a vendor's specimens as follows:

Metallurgical Test Program

Specimen Location	Test Type	Specimen Orientation
Hub	High Temperature Tensile	1 Radial 1 Tangential
	High Temperature Creep-Rupture	2 Radial 2 Tangential
Hub/Blade	High Temperature Tensile	2 Radial
	High Temperature Creep-Rupture	4 Radial
Blade Exducer	High Temperature Tensile	2 Radial
	High Temperature Creep-Rupture	2 Radial
Blade Star	High Temperature Tensile	4 Radial
	High Temperature Creep-Rupture	4 Radial

F. TASK 6 - COLD FLOW TESTS

Water Flow Rig Completed - Shakedown Started

Fabrication of the water flow rig was delayed (seven weeks) more than any other item in the program by the UAW-CIO strike at UACL. However, all parts have been fabricated and the rig was assembled in October. Shakedown tests were started in late October, and the target date for the initial water rig tests has been rescheduled for November. This slippage is not expected to have a serious effect on the overall program schedule.

Cold Flow Tests Delayed

Cold flow tests have been delayed by about two weeks as a result of strike-caused delays in nozzle procurement. Start of cold flow rig assembly has been rescheduled for late January 1968. As this item can affect the overall completion date, every effort will be made to recover some of the lost time.

SECTION III
WORK PLANNED FOR NEXT REPORT PERIOD

The aerodynamic/structural/heat transfer cycle will continue for the hot nozzle section, the front and rear shrouds, and the hot rotor.

The hot test rig will be studied in detail for part-load performance and the test stand control system.

The first rotor and nozzle specimens for the Fabrication Study are expected near the end of the next monthly report period.

Water rig shakedown tests will be completed, and visual observations of the rotor flow pattern will begin.

FD 20818

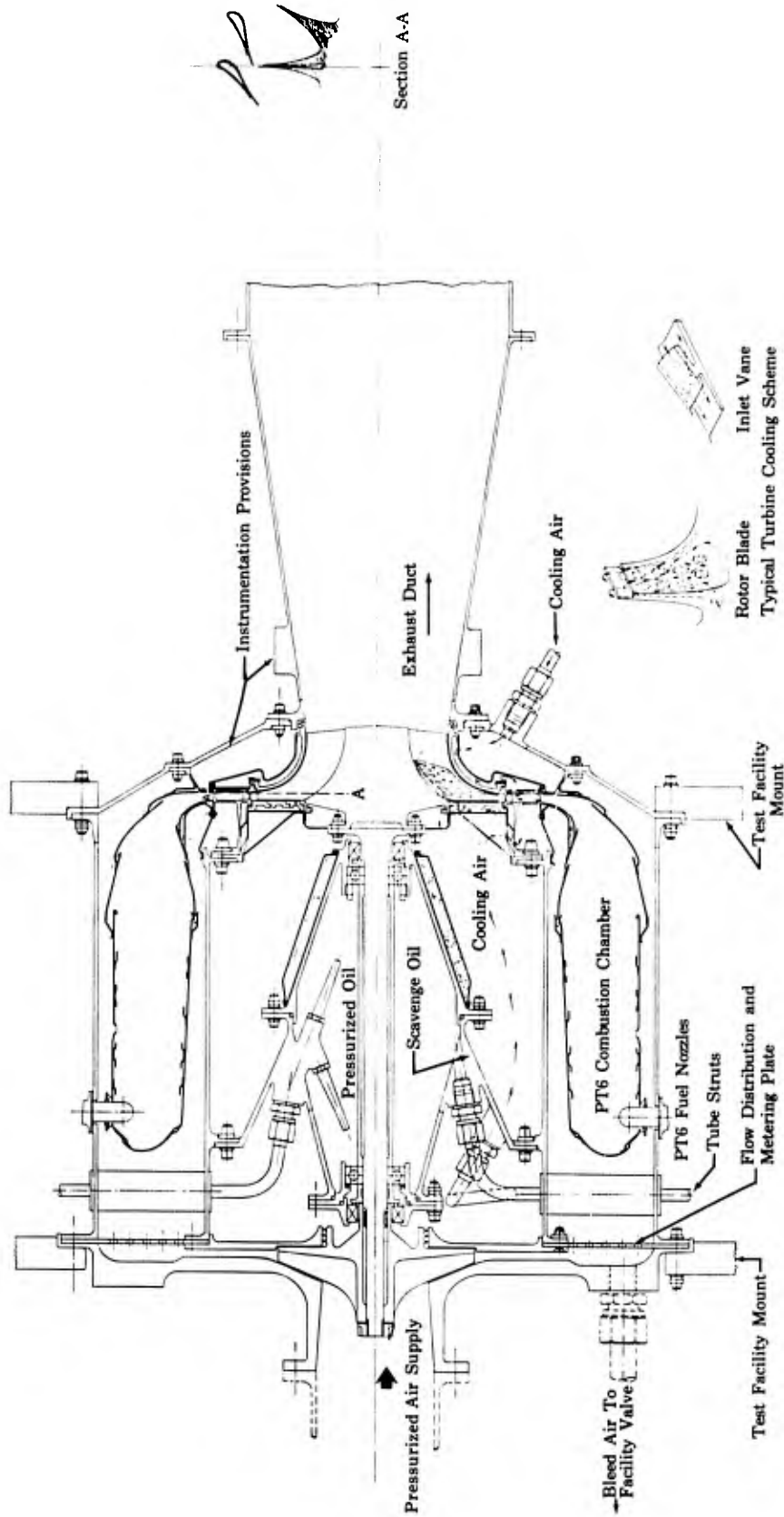
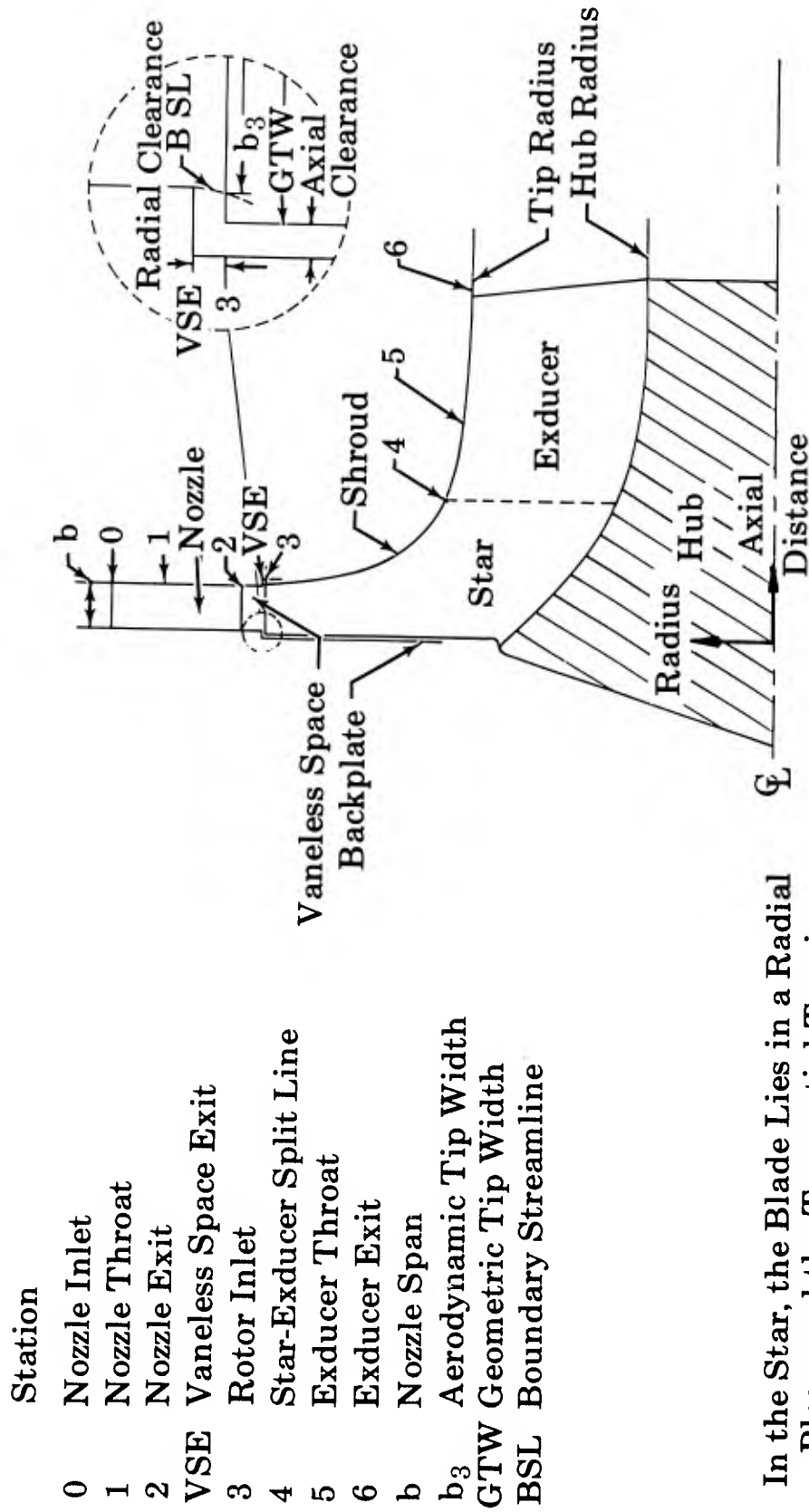


Figure 1. Control Layout High Temperature Radial Turbine Test Rig



In the Star, the Blade Lies in a Radial Plane and the Tangential Turning is Done Only in the Exducer Portion

- Station
- 0 Nozzle Inlet
- 1 Nozzle Throat
- 2 Nozzle Exit
- VSE Vaneless Space Exit
- 3 Rotor Inlet
- 4 Star-Exducer Split Line
- 5 Exducer Throat
- 6 Exducer Exit
- b Nozzle Span
- b₃ Aerodynamic Tip Width
- GTW Geometric Tip Width
- BSL Boundary Streamline

Figure 2. Radial Turbine Rotor Terminology

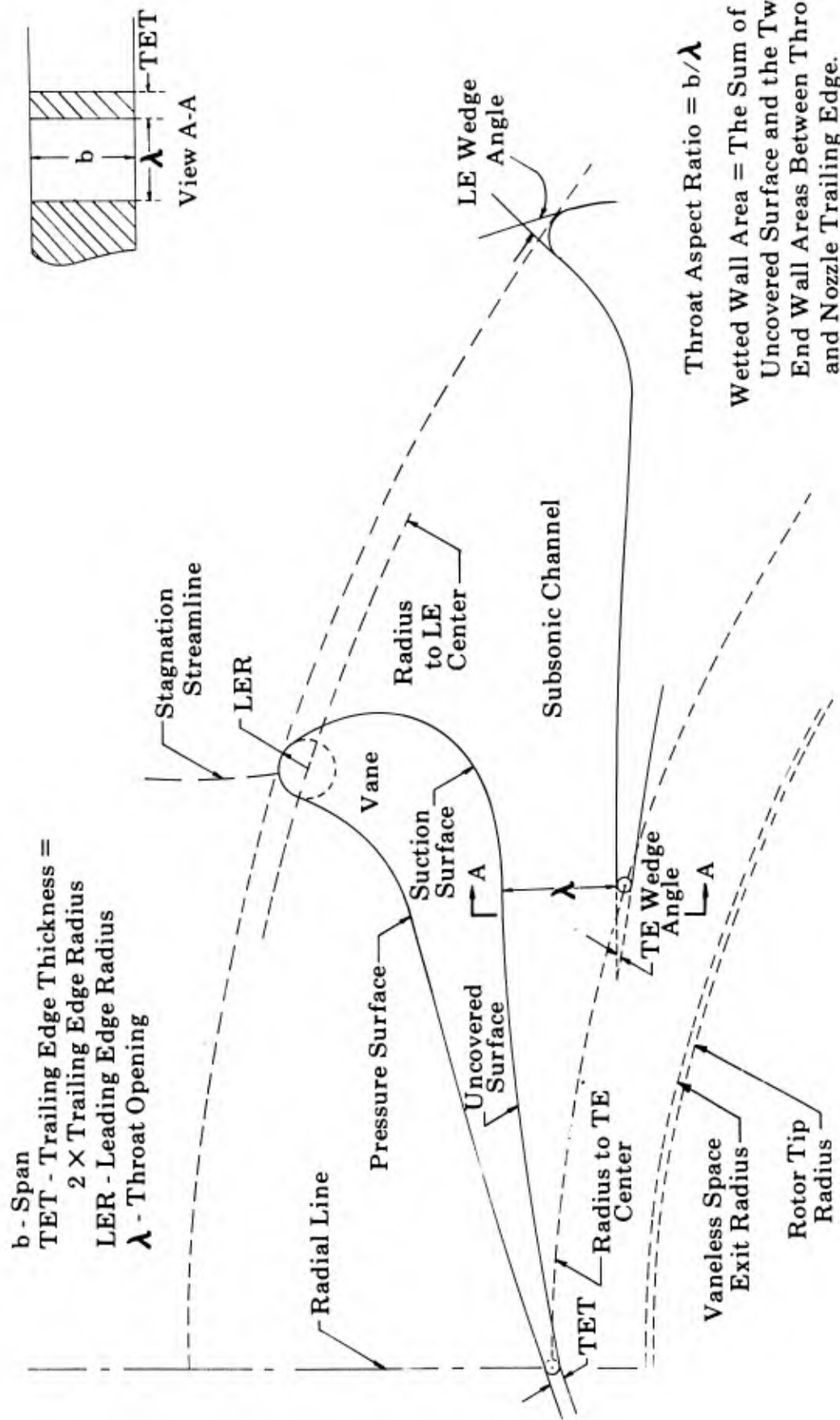


Figure 3. Radial Turbine Nozzle Terminology

FD 23253

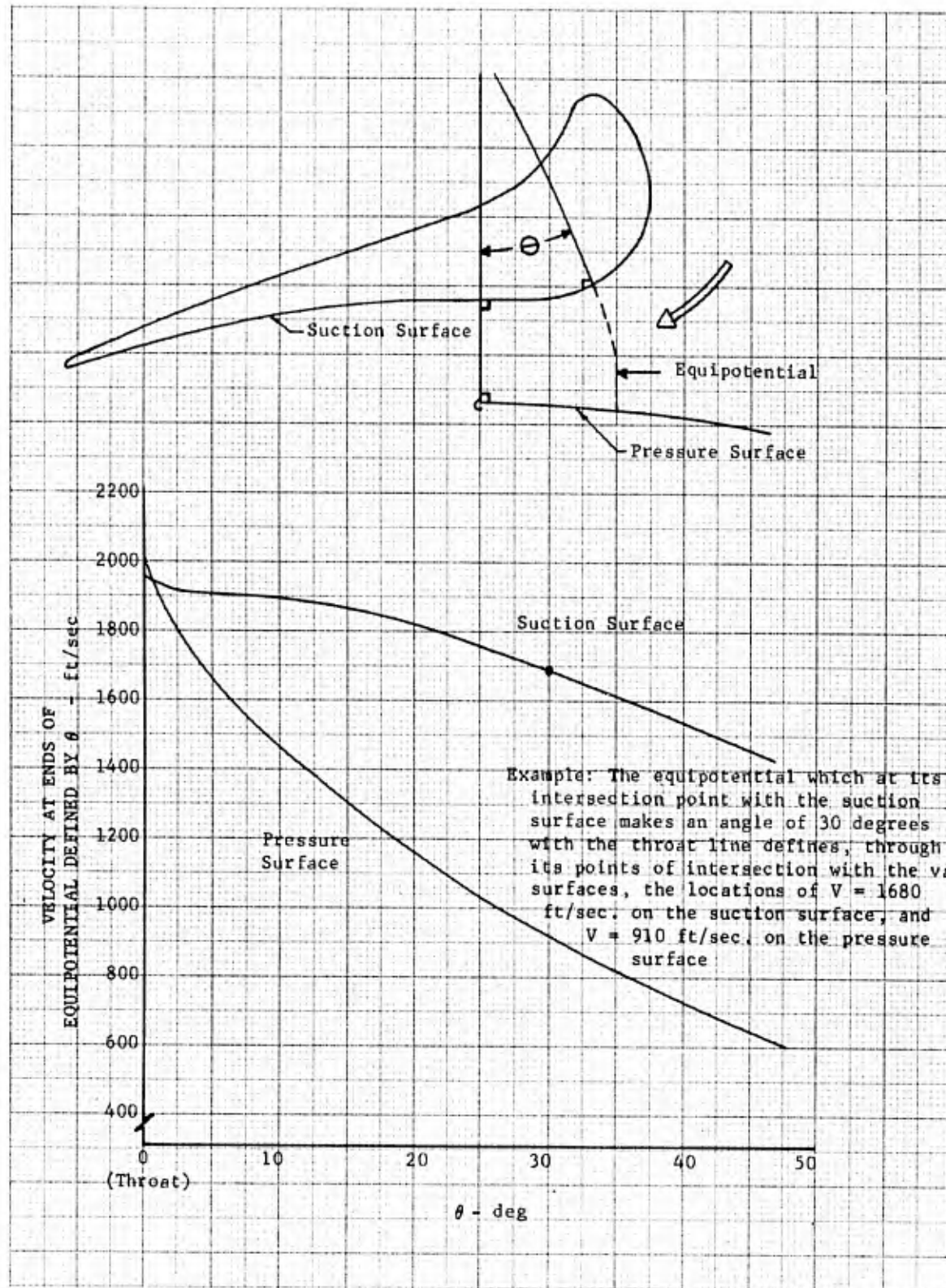


Figure 4. Calculated Channel Velocity Distribution is Identical for All Cold Flow Nozzles

DF 60055

FD 23254

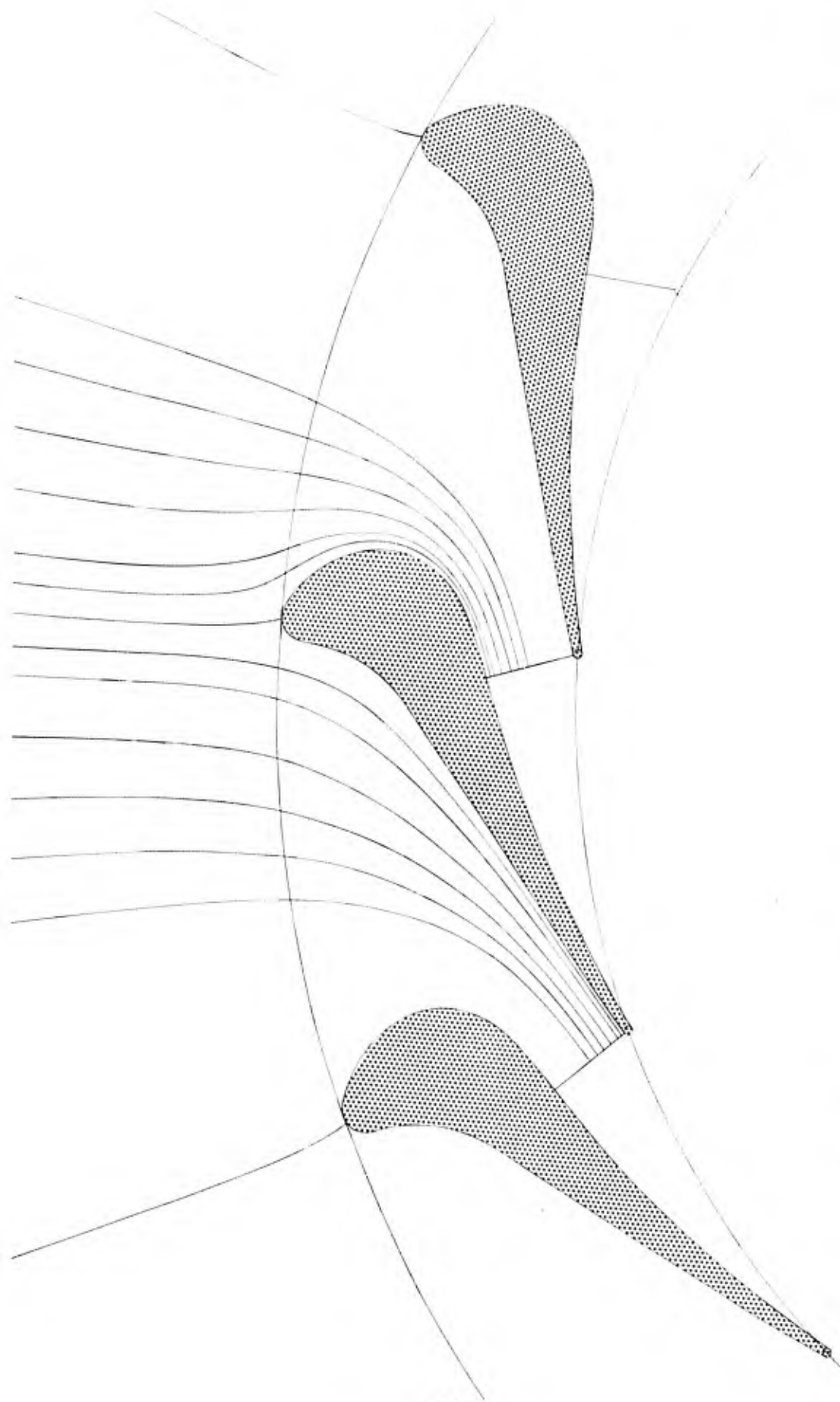


Figure 5. 15-Vane Nozzle Streamline Pattern

FD 23255

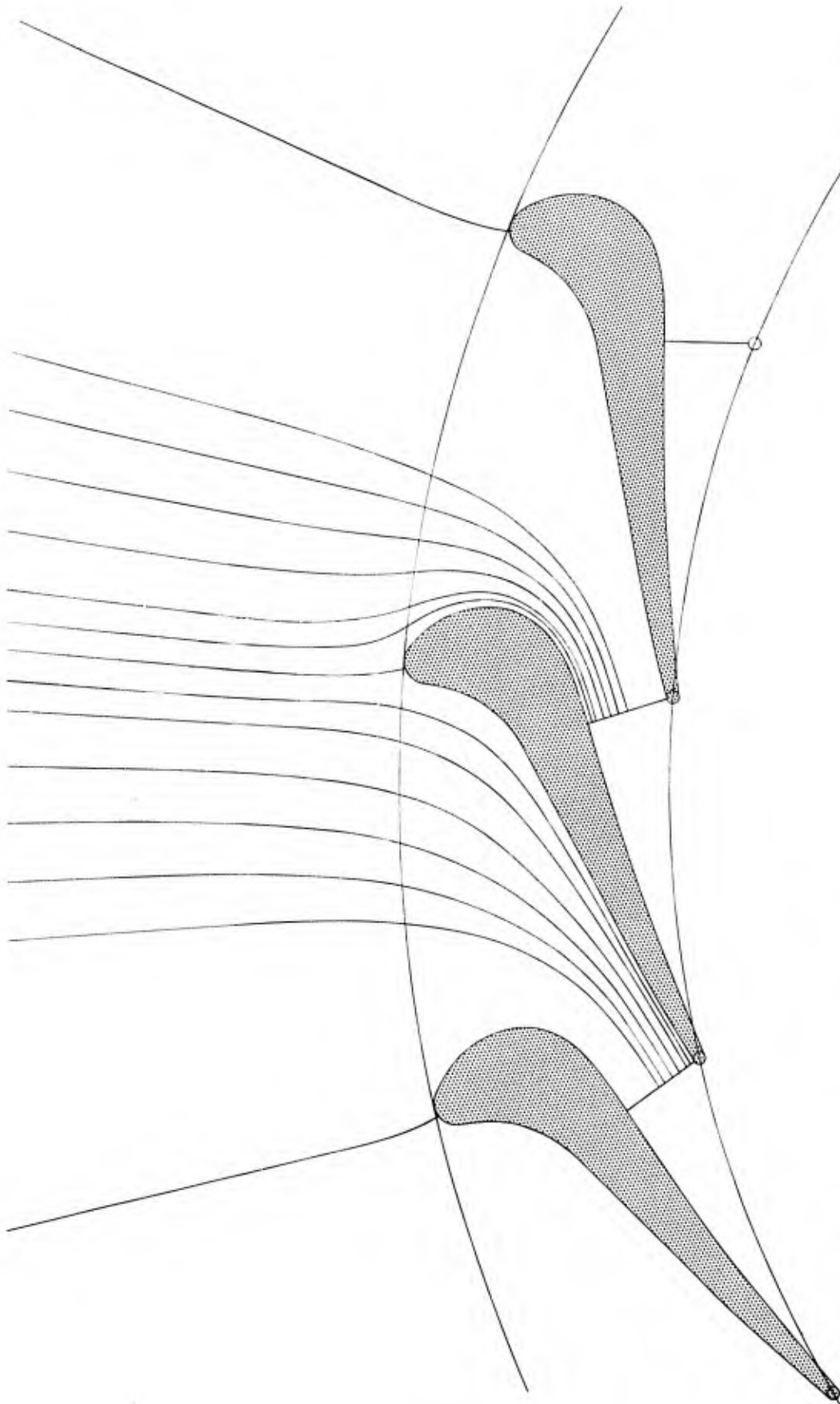


Figure 6. 20-Vane Nozzle Streamline Pattern

FD 23256

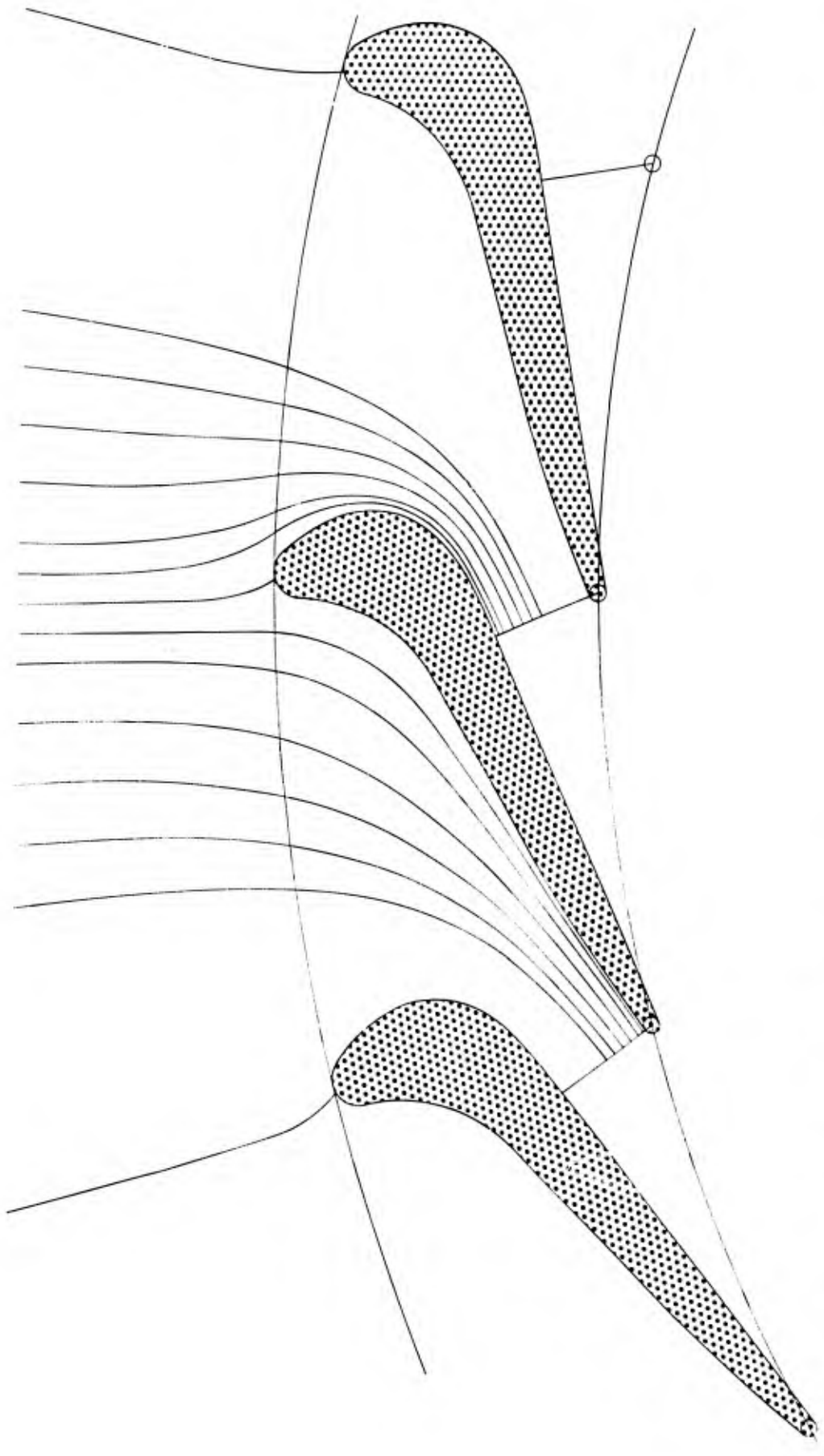


Figure 7. 25-Vane Nozzle Streamline Pattern

FD 23257

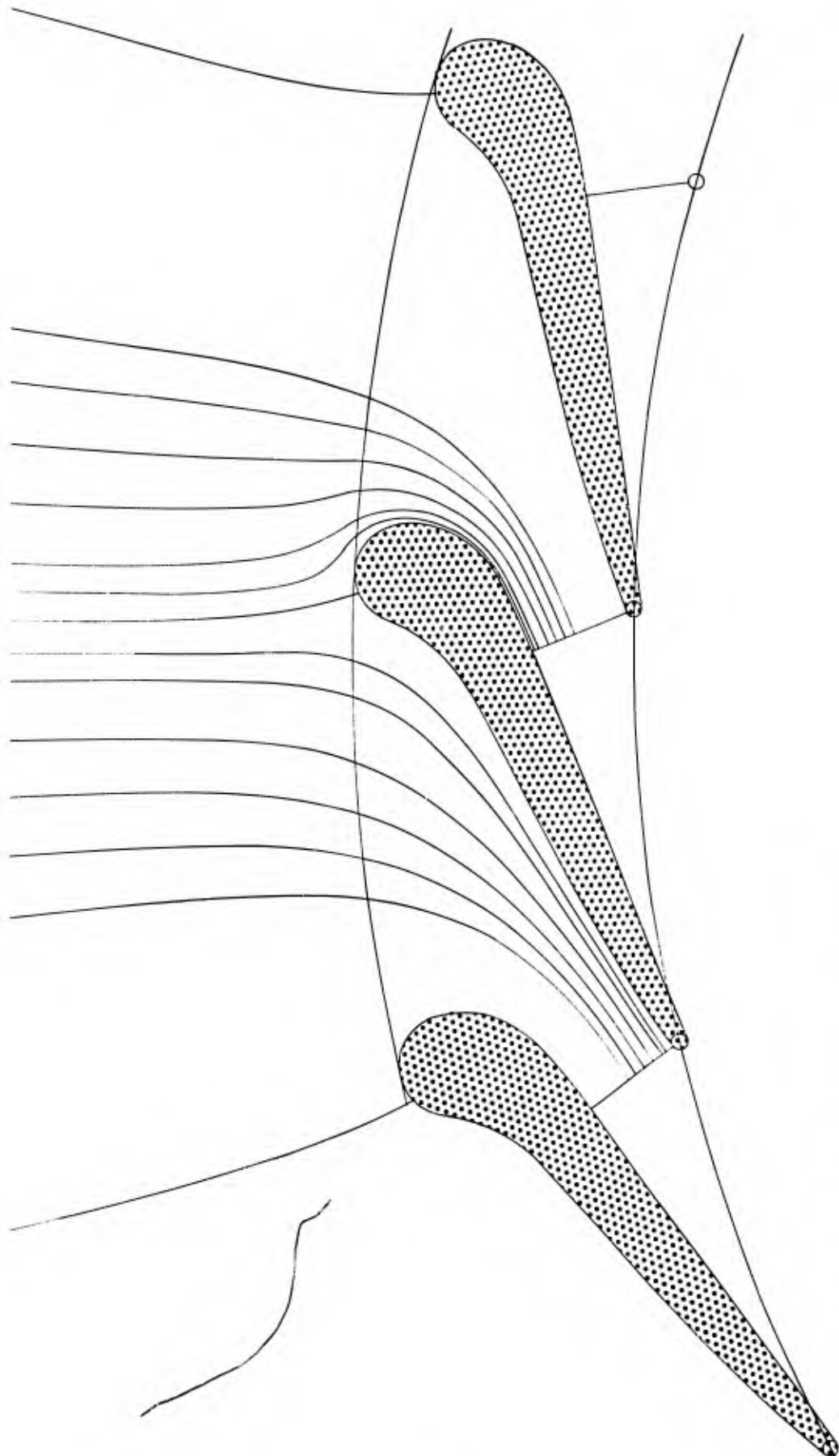


Figure 8. 25-Modified-Vane Streamline Pattern (1)

FD 23258

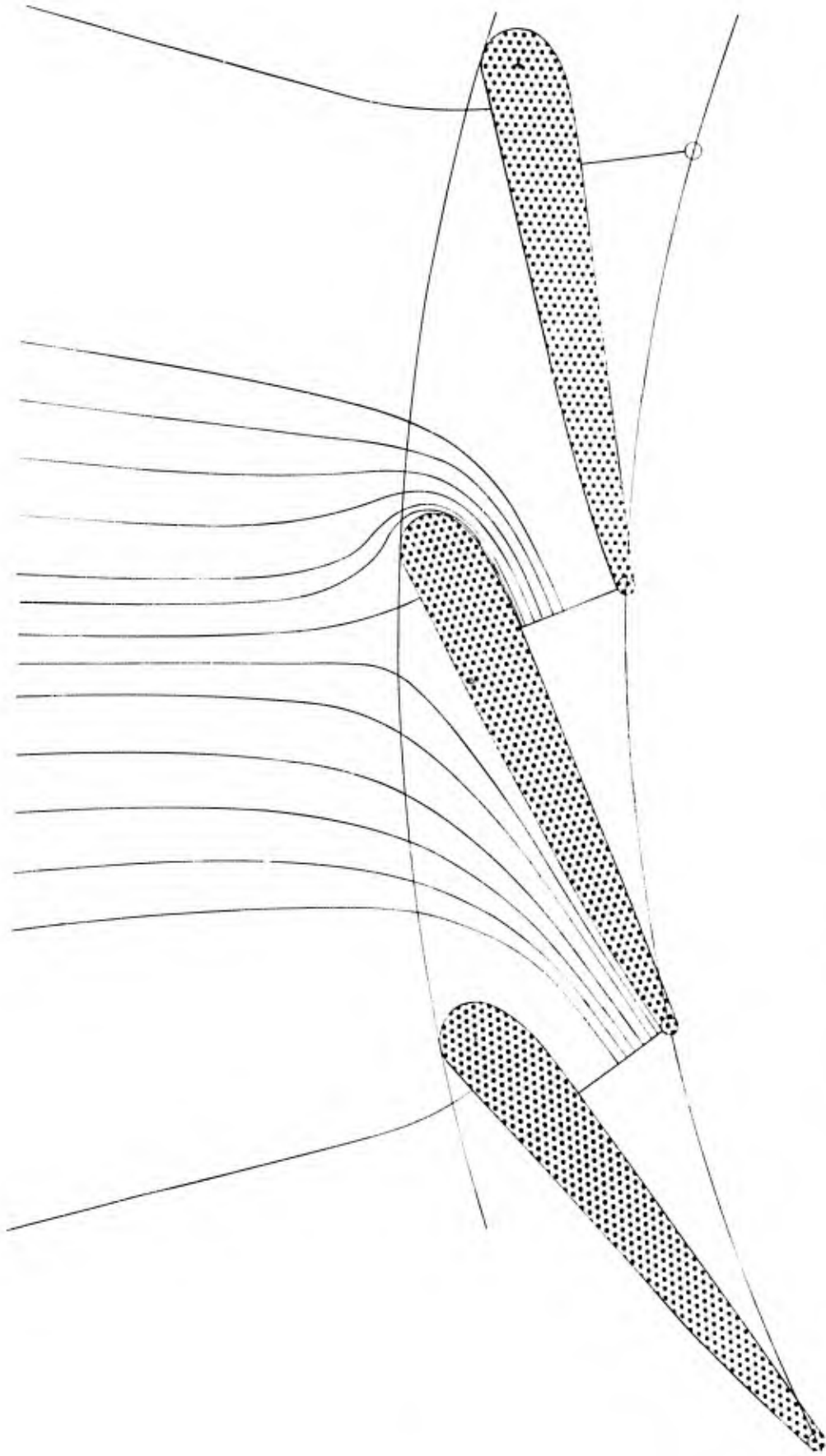
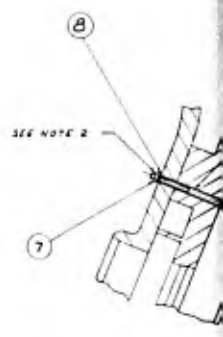
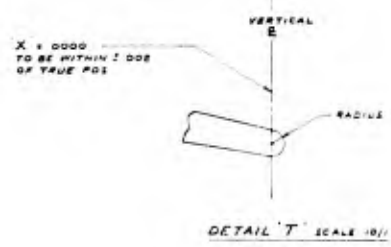
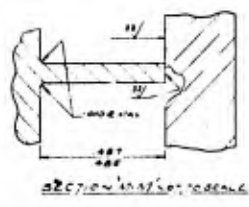
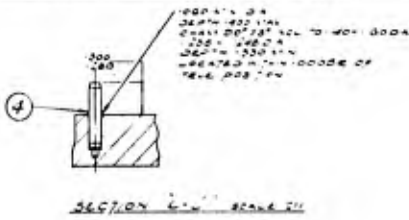


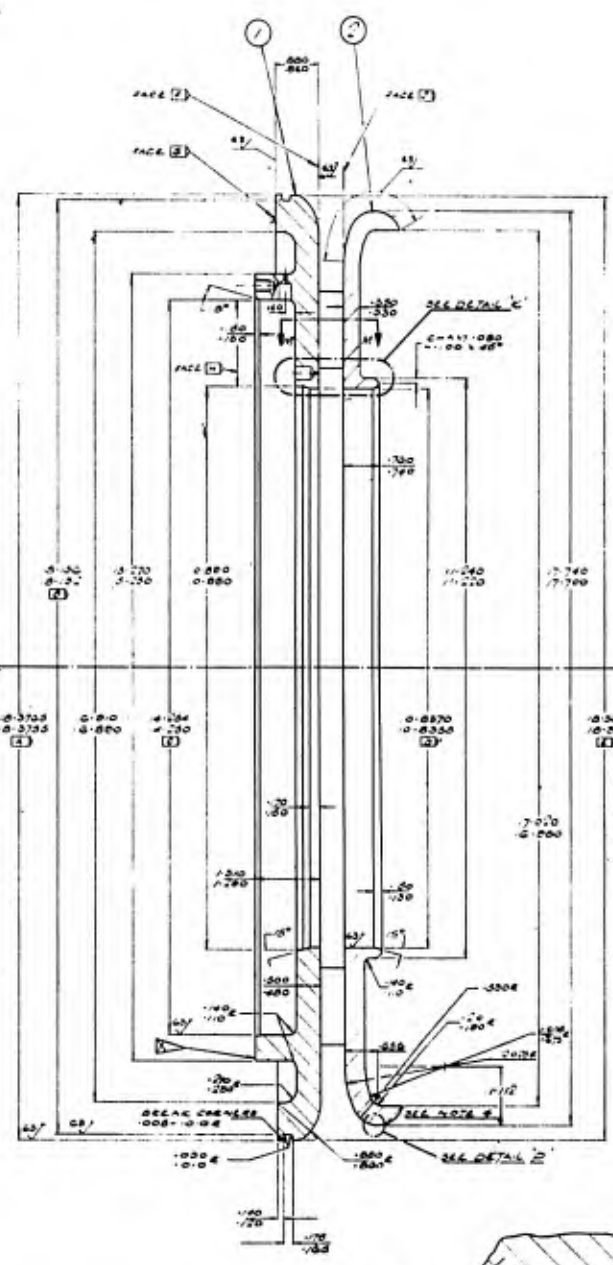
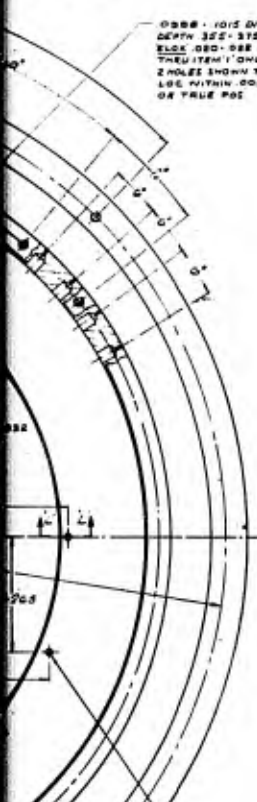
Figure 9. 25-Modified-Vane Streamline Pattern (2)



LOCATED
2.000 ± .001

70 - 113 DIA
DEPTH .332 - .352
HOLE DIA .022 DIA
THRU ITEM 1 ONLY
2 HOLES SHOWN THUS
LOC WITHIN .002 OF
TRUE POS

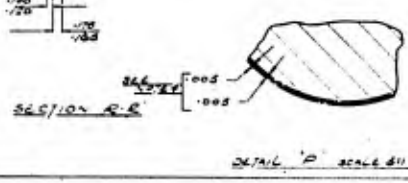
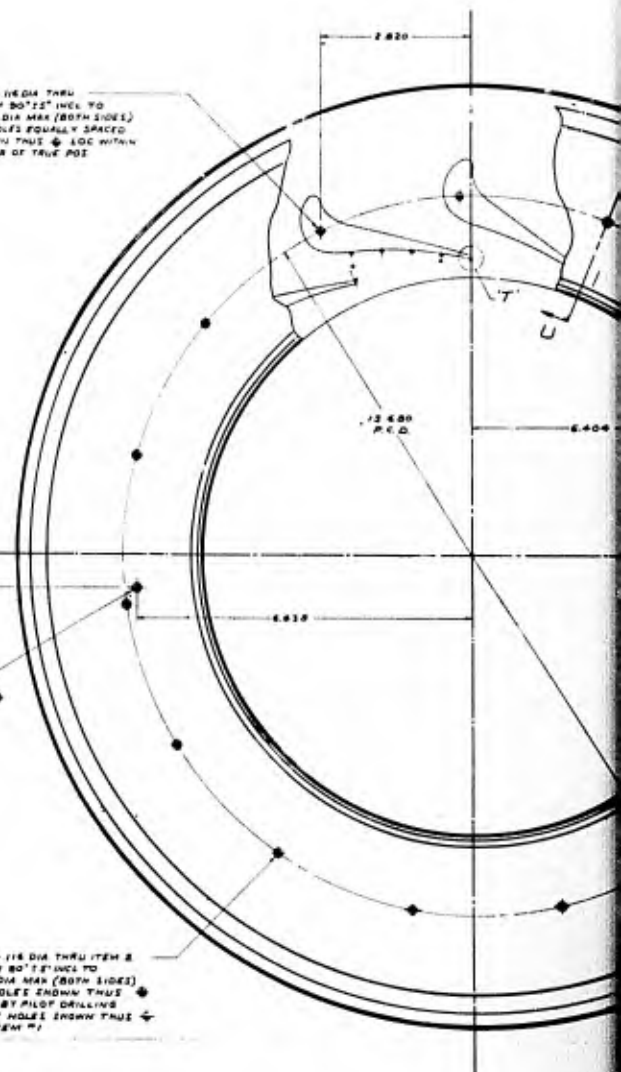
.008 - .015 DIA
DEPTH .332 - .312
HOLE DIA .022 DIA
THRU ITEM 1 ONLY
2 HOLES SHOWN THUS
LOC WITHIN .002 OF
TRUE POS



.113 - .116 DIA THRU
CHAM .80 ± .02 INCL TO
.122 DIA MAX (BOTH SIDES)
15 HOLES EQUALLY SPACED
SHOWN THUS LOC WITHIN
.002 OF TRUE POS

.042 - .044 DIA
THRU ITEM 2 ONLY
2 HOLES SHOWN THUS
LOC WITHIN .002 OF
TRUE POS

.113 - .116 DIA THRU ITEM 2
CHAM .80 ± .02 INCL TO
.122 DIA MAX (BOTH SIDES)
15 HOLES EQUALLY SPACED
LOC BY FILED DRILLING
THRU HOLES SHOWN THUS
IN ITEM 1



DETAIL P SCALE 5X

B.

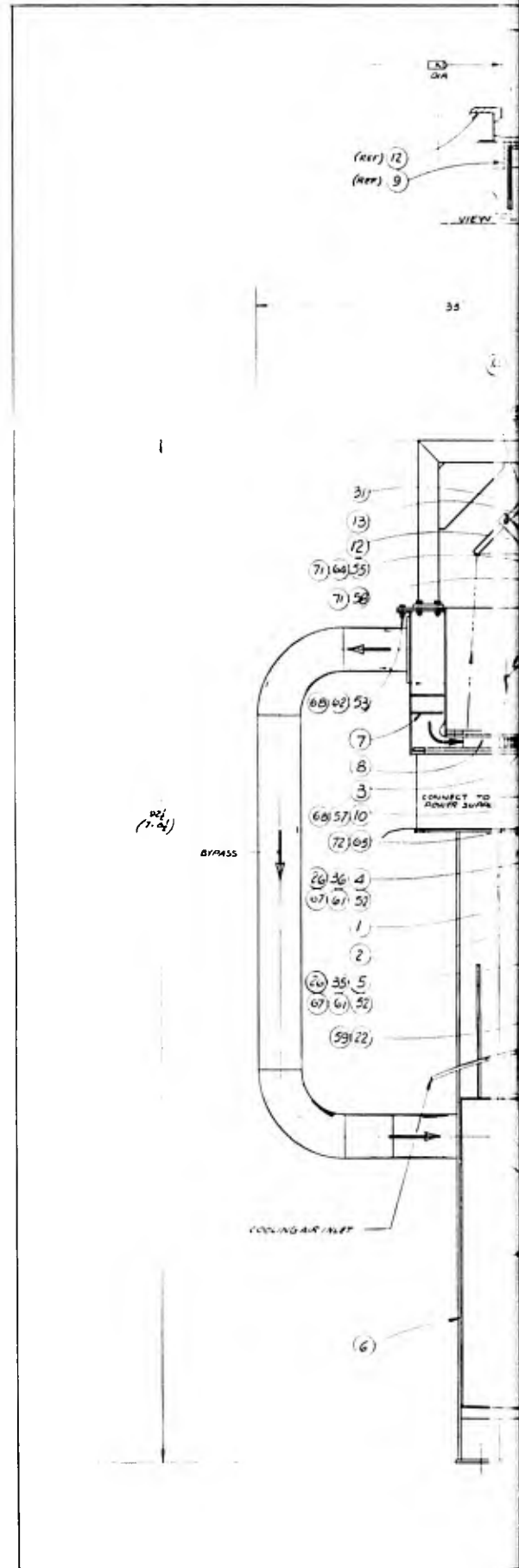
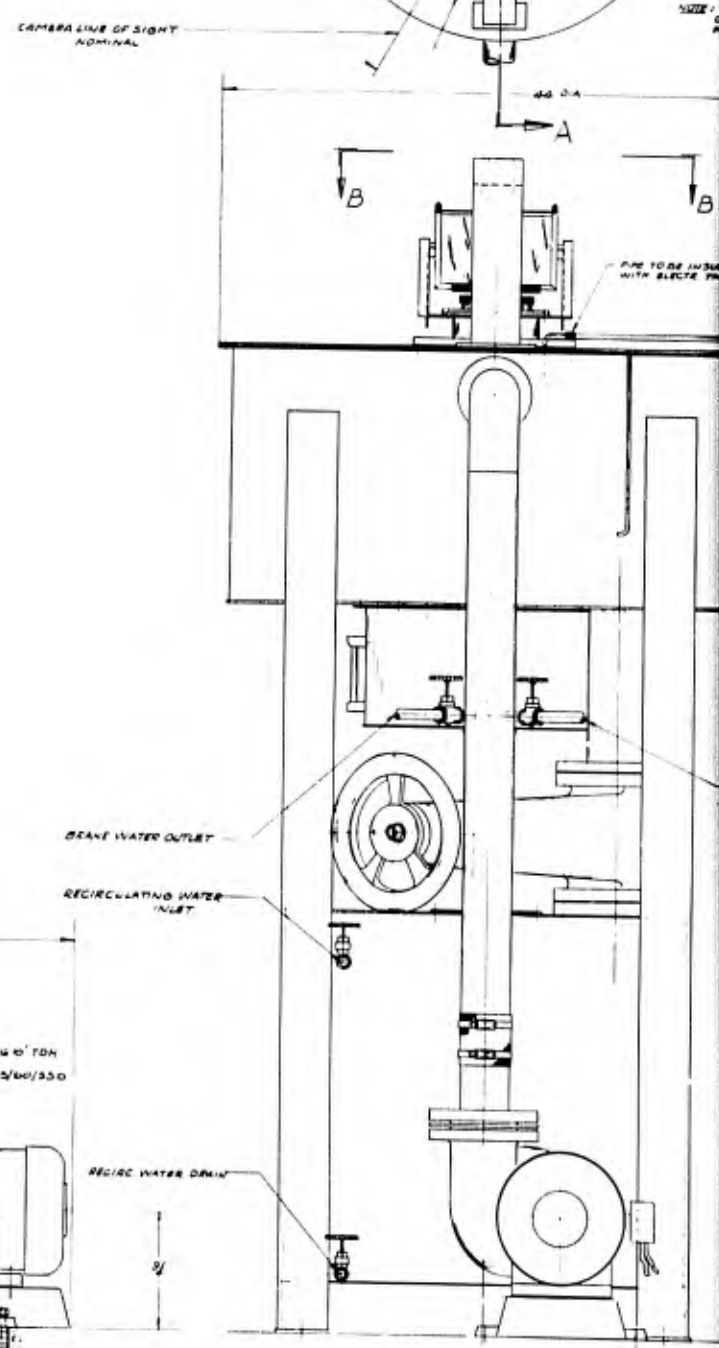
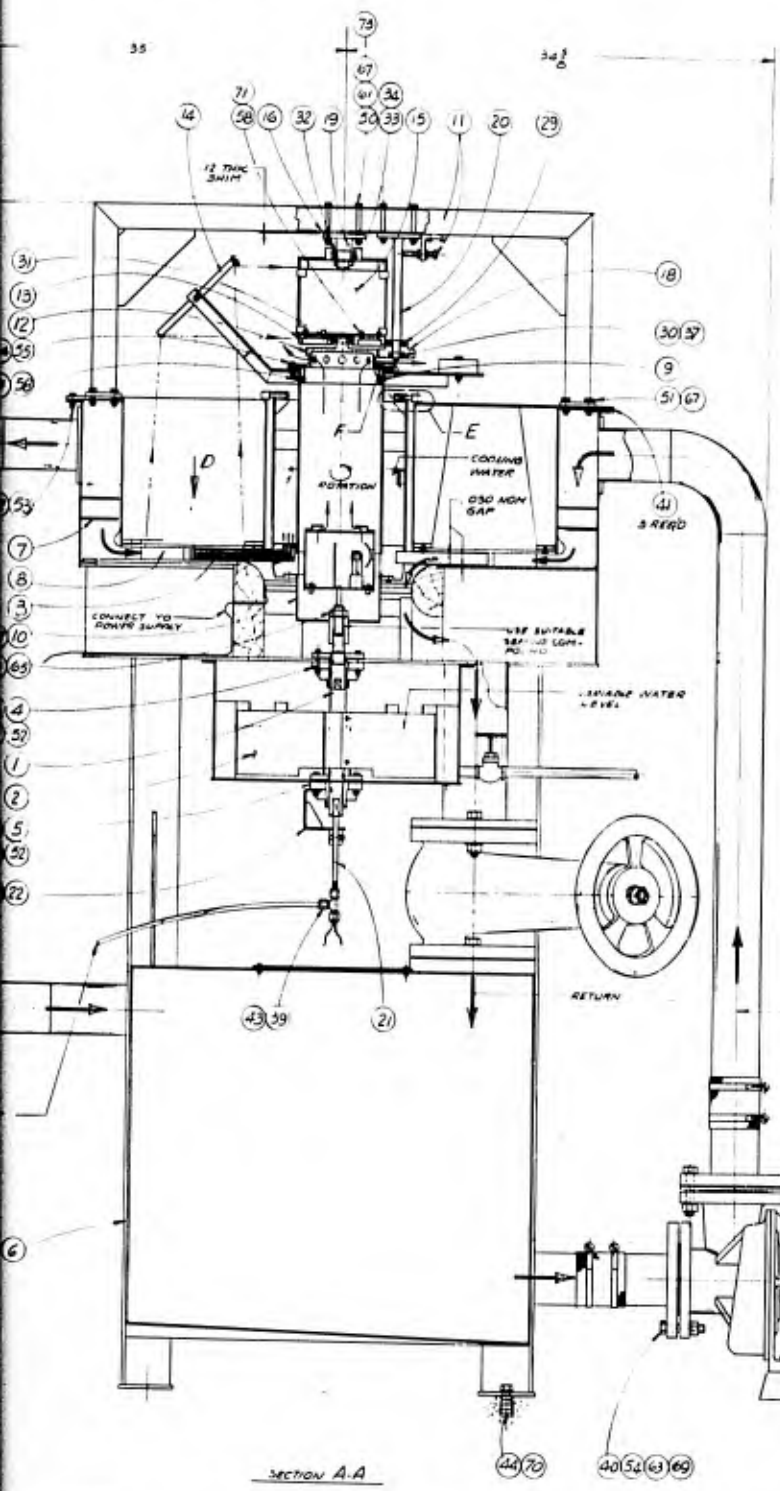
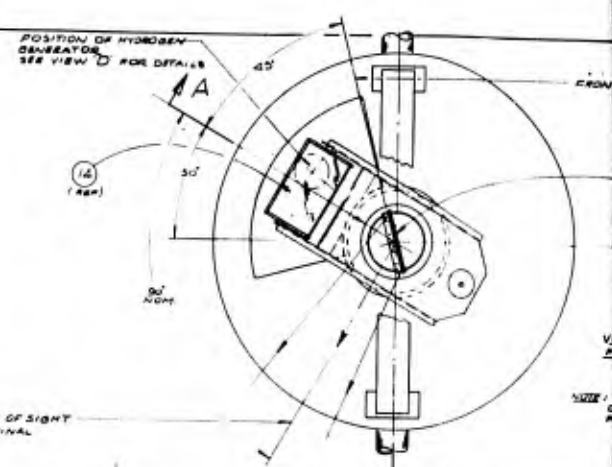
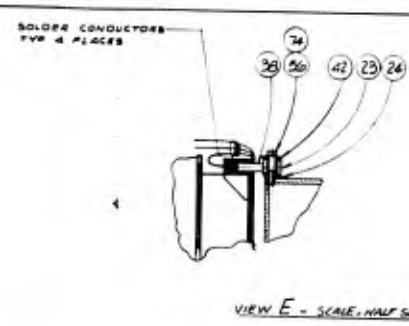
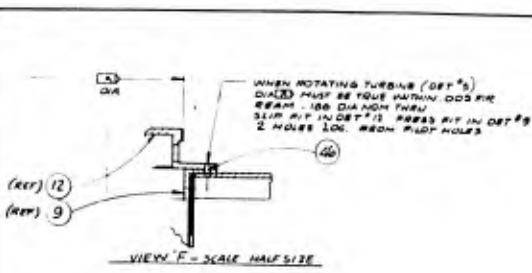
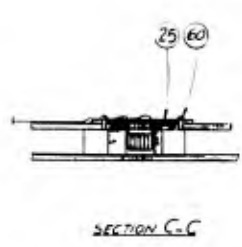
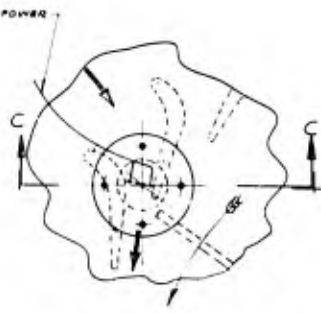
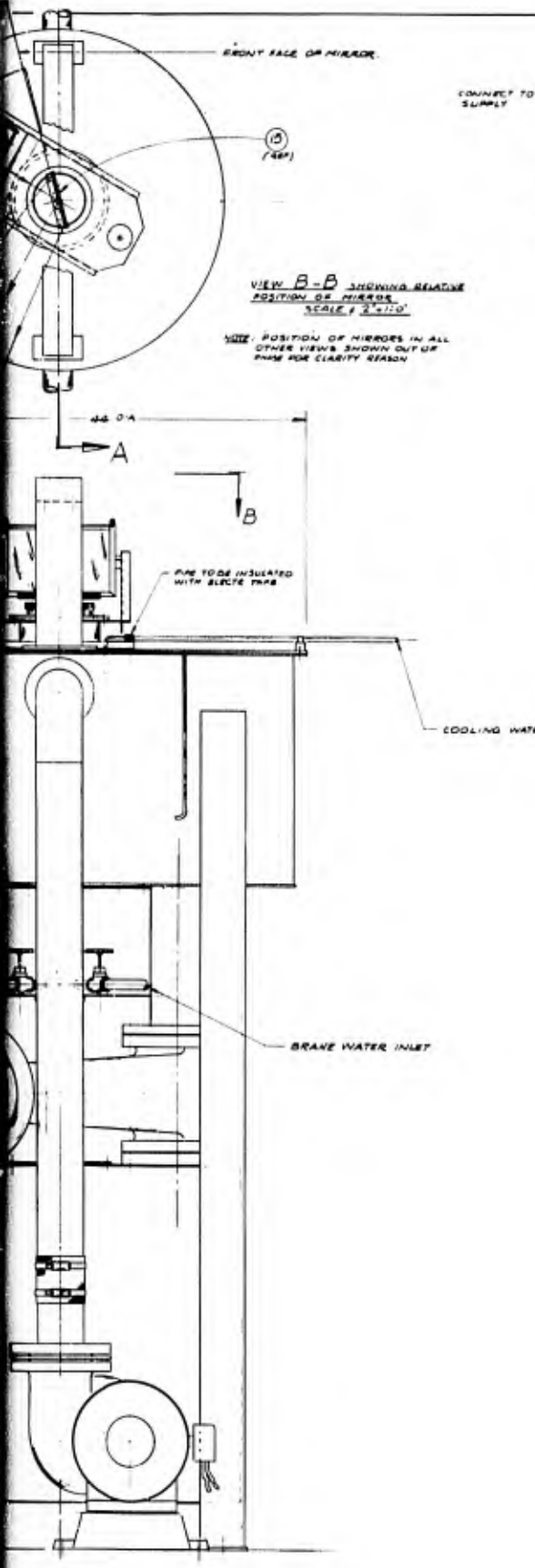


Figure 14. Water Visualization Rig

A.



B.



NO	DESCRIPTION	QTY	MATERIAL	REMARKS
73	WASHER PLAIN	4	1/4 10 NOM	
74	WASHER PLAIN	0	3/8 10 NOM	
75	WASHER SPRING LOCK	1	1/8 10 NOM	
76		12	1/8 10 NOM	
77		0	3/8 10 NOM	
78		24	3/8 10 NOM	
79		30	1/4 0 NOM	
80	WASHER SPRING LOCK	24	3/8 10 NOM	
81	NUT - JAM	1	3/8-14 UNF	
82	NUT - REG	4	3/8-14 NF	
83	NUT - REG	16	3/8-11 NC	
84	NUT - REG	24	3/8-20 NC	
85	NUT - REG	10	3/8-16 NC	
86	SCREW - RND HD	4	3/8-24 NC X 3/8 LONG	
87	SET SCREW	2	1/4-20 NC X 1/2 LONG	
88	BOLT - SOCKET HD	8	3/8-24 NC X 1/2 LONG	
89	BOLT - HEX HD	6	1/2-20 NC X 1/2 LONG	
90		4	3/8-24 NC X 1/2 LONG	
91		10	3/8-24 NC X 1/2 LONG	
92		24	3/8-24 NC X 1/2 LONG	
93		5	3/8-24 NC X 1/2 LONG	
94		6	3/8-24 NC X 1/2 LONG	
95	BOLT - HEX HD	6	3/8-24 NC X 1/2 LONG	
96				
97				
98				
99				
100				
101				
102				
103				
104				
105				
106				
107				
108				
109				
110				
111				
112				
113				
114				
115				
116				
117				
118				
119				
120				
121				
122				
123				
124				
125				
126				
127				
128				
129				
130				
131				
132				
133				
134				
135				
136				
137				
138				
139				
140				
141				
142				
143				
144				
145				
146				
147				
148				
149				
150				
151				
152				
153				
154				
155				
156				
157				
158				
159				
160				
161				
162				
163				
164				
165				
166				
167				
168				
169				
170				
171				
172				
173				
174				
175				
176				
177				
178				
179				
180				
181				
182				
183				
184				
185				
186				
187				
188				
189				
190				
191				
192				
193				
194				
195				
196				
197				
198				
199				
200				

101				
102				
103				
104				
105				
106				
107				
108				
109				
110				
111				
112				
113				
114				
115				
116				
117				
118				
119				
120				
121				
122				
123				
124				
125				
126				
127				
128				
129				
130				
131				
132				
133				
134				
135				
136				
137				
138				
139				
140				
141				
142				
143				
144				
145				
146				
147				
148				
149				
150				
151				
152				
153				
154				
155				
156				
157				
158				
159				
160				
161				
162				
163				
164				
165				
166				
167				
168				
169				
170				
171				
172				
173				
174				
175				
176				
177				
178				
179				
180				
181				
182				
183				
184				
185				
186				
187				
188				
189				
190				
191				
192				
193				
194				
195				
196				
197				
198				
199				
200				

EFD-31704

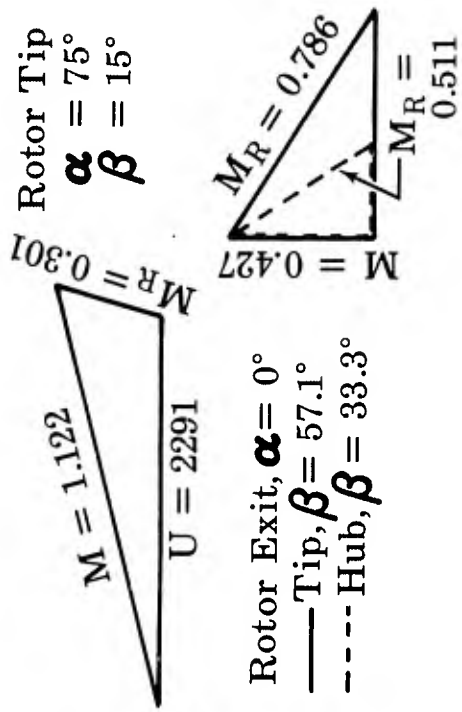
7	SCREW ASSY	1	EFD-31711	
8	MAIN BEARING WASHING	1	EFD-31712	
9	SHAFT SEAL PLATE WASHING	1	EFD-31713	
10	SHAFT SEAL PLATE WASHING	1	EFD-31714	
11	SHAFT SEAL PLATE WASHING	1	EFD-31715	
12	SHAFT SEAL PLATE WASHING	1	EFD-31716	
13	SHAFT SEAL PLATE WASHING	1	EFD-31717	
14	SHAFT SEAL PLATE WASHING	1	EFD-31718	
15	SHAFT SEAL PLATE WASHING	1	EFD-31719	
16	SHAFT SEAL PLATE WASHING	1	EFD-31720	
17	SHAFT SEAL PLATE WASHING	1	EFD-31721	
18	SHAFT SEAL PLATE WASHING	1	EFD-31722	
19	SHAFT SEAL PLATE WASHING	1	EFD-31723	
20	SHAFT SEAL PLATE WASHING	1	EFD-31724	
21	SHAFT SEAL PLATE WASHING	1	EFD-31725	
22	SHAFT SEAL PLATE WASHING	1	EFD-31726	
23	SHAFT SEAL PLATE WASHING	1	EFD-31727	
24	SHAFT SEAL PLATE WASHING	1	EFD-31728	
25	SHAFT SEAL PLATE WASHING	1	EFD-31729	
26	SHAFT SEAL PLATE WASHING	1	EFD-31730	
27	SHAFT SEAL PLATE WASHING	1	EFD-31731	
28	SHAFT SEAL PLATE WASHING	1	EFD-31732	
29	SHAFT SEAL PLATE WASHING	1	EFD-31733	
30	SHAFT SEAL PLATE WASHING	1	EFD-31734	
31	SHAFT SEAL PLATE WASHING	1	EFD-31735	
32	SHAFT SEAL PLATE WASHING	1	EFD-31736	
33	SHAFT SEAL PLATE WASHING	1	EFD-31737	
34	SHAFT SEAL PLATE WASHING	1	EFD-31738	
35	SHAFT SEAL PLATE WASHING	1	EFD-31739	
36	SHAFT SEAL PLATE WASHING	1	EFD-31740	
37	SHAFT SEAL PLATE WASHING	1	EFD-31741	
38	SHAFT SEAL PLATE WASHING	1	EFD-31742	
39	SHAFT SEAL PLATE WASHING	1	EFD-31743	
40	SHAFT SEAL PLATE WASHING	1	EFD-31744	
41	SHAFT SEAL PLATE WASHING	1	EFD-31745	
42	SHAFT SEAL PLATE WASHING	1	EFD-31746	
43	SHAFT SEAL PLATE WASHING	1	EFD-31747	
44	SHAFT SEAL PLATE WASHING	1	EFD-31748	
45	SHAFT SEAL PLATE WASHING	1	EFD-31749	
46	SHAFT SEAL PLATE WASHING	1	EFD-31750	
47	SHAFT SEAL PLATE WASHING	1	EFD-31751	
48	SHAFT SEAL PLATE WASHING	1	EFD-31752	
49	SHAFT SEAL PLATE WASHING	1	EFD-31753	
50	SHAFT SEAL PLATE WASHING	1	EFD-31754	
51	SHAFT SEAL PLATE WASHING	1	EFD-31755	
52	SHAFT SEAL PLATE WASHING	1	EFD-31756	
53	SHAFT SEAL PLATE WASHING	1	EFD-31757	
54	SHAFT SEAL PLATE WASHING	1	EFD-31758	
55	SHAFT SEAL PLATE WASHING	1	EFD-31759	
56	SHAFT SEAL PLATE WASHING	1	EFD-31760	
57	SHAFT SEAL PLATE WASHING	1	EFD-31761	
58	SHAFT SEAL PLATE WASHING	1	EFD-31762	
59	SHAFT SEAL PLATE WASHING	1	EFD-31763	
60	SHAFT SEAL PLATE WASHING	1	EFD-31764	
61	SHAFT SEAL PLATE WASHING	1	EFD-31765	
62	SHAFT SEAL PLATE WASHING	1	EFD-31766	
63	SHAFT SEAL PLATE WASHING	1	EFD-31767	
64	SHAFT SEAL PLATE WASHING	1	EFD-31768	
65	SHAFT SEAL PLATE WASHING	1	EFD-31769	
66	SHAFT SEAL PLATE WASHING	1	EFD-31770	
67	SHAFT SEAL PLATE WASHING	1	EFD-31771	
68	SHAFT SEAL PLATE WASHING	1	EFD-31772	
69	SHAFT SEAL PLATE WASHING	1	EFD-31773	
70	SHAFT SEAL PLATE WASHING	1	EFD-31774	
71	SHAFT SEAL PLATE WASHING	1	EFD-31775	
72	SHAFT SEAL PLATE WASHING	1	EFD-31776	
73	SHAFT SEAL PLATE WASHING	1	EFD-31777	
74	SHAFT SEAL PLATE WASHING	1	EFD-31778	
75	SHAFT SEAL PLATE WASHING	1	EFD-31779	
76	SHAFT SEAL PLATE WASHING	1	EFD-31780	
77	SHAFT SEAL PLATE WASHING	1	EFD-31781	
78	SHAFT SEAL PLATE WASHING	1	EFD-31782	
79	SHAFT SEAL PLATE WASHING	1	EFD-31783	
80	SHAFT SEAL PLATE WASHING	1	EFD-31784	
81	SHAFT SEAL PLATE WASHING	1	EFD-31785	
82	SHAFT SEAL PLATE WASHING	1	EFD-31786	
83	SHAFT SEAL PLATE WASHING	1	EFD-31787	
84	SHAFT SEAL PLATE WASHING	1	EFD-31788	
85	SHAFT SEAL PLATE WASHING	1	EFD-31789	
86	SHAFT SEAL PLATE WASHING	1	EFD-31790	
87	SHAFT SEAL PLATE WASHING	1	EFD-31791	
88	SHAFT SEAL PLATE WASHING	1	EFD-31792	
89	SHAFT SEAL PLATE WASHING	1	EFD-31793	
90	SHAFT SEAL PLATE WASHING	1	EFD-31794	
91	SHAFT SEAL PLATE WASHING	1	EFD-31795	
92	SHAFT SEAL PLATE WASHING	1	EFD-31796	
93	SHAFT SEAL PLATE WASHING	1	EFD-31797	
94	SHAFT SEAL PLATE WASHING	1	EFD-31798	
95	SHAFT SEAL PLATE WASHING	1	EFD-31799	
96	SHAFT SEAL PLATE WASHING	1	EFD-31800	
97	SHAFT SEAL PLATE WASHING	1	EFD-31801	
98	SHAFT SEAL PLATE WASHING	1	EFD-31802	
99	SHAFT SEAL PLATE WASHING	1	EFD-31803	
100	SHAFT SEAL PLATE WASHING	1	EFD-31804	

EXPERIMENTAL ENGINEERING DEPARTMENT
CANADIAN PRATT & WHITNEY AIRCRAFT DIVISION
UNITED AIRCRAFT OF CANADA LIMITED
JACQUES CARTIER, QUEBEC, CANADA

WATER ANALOGY RIG
RADIAL TURBINE

DESIGN CHECKED APPROVED
EFD-31704

C.



VELOCITY TRIANGLES

- $W_{inlet} = 5.00$ lb/sec
- $T_{IT} = 2760^\circ R$
- $P_{inlet} = 257.5$ psia
- $N = 67,000$ rpm
- $N_s = 64.8$
- $PR = 5.165$
- $\Delta H = 226.0$ Btu/lb
- $\eta_{TT} = 0.875$
- $\phi_N^2 = 0.940$
- $\eta_R = 0.757$

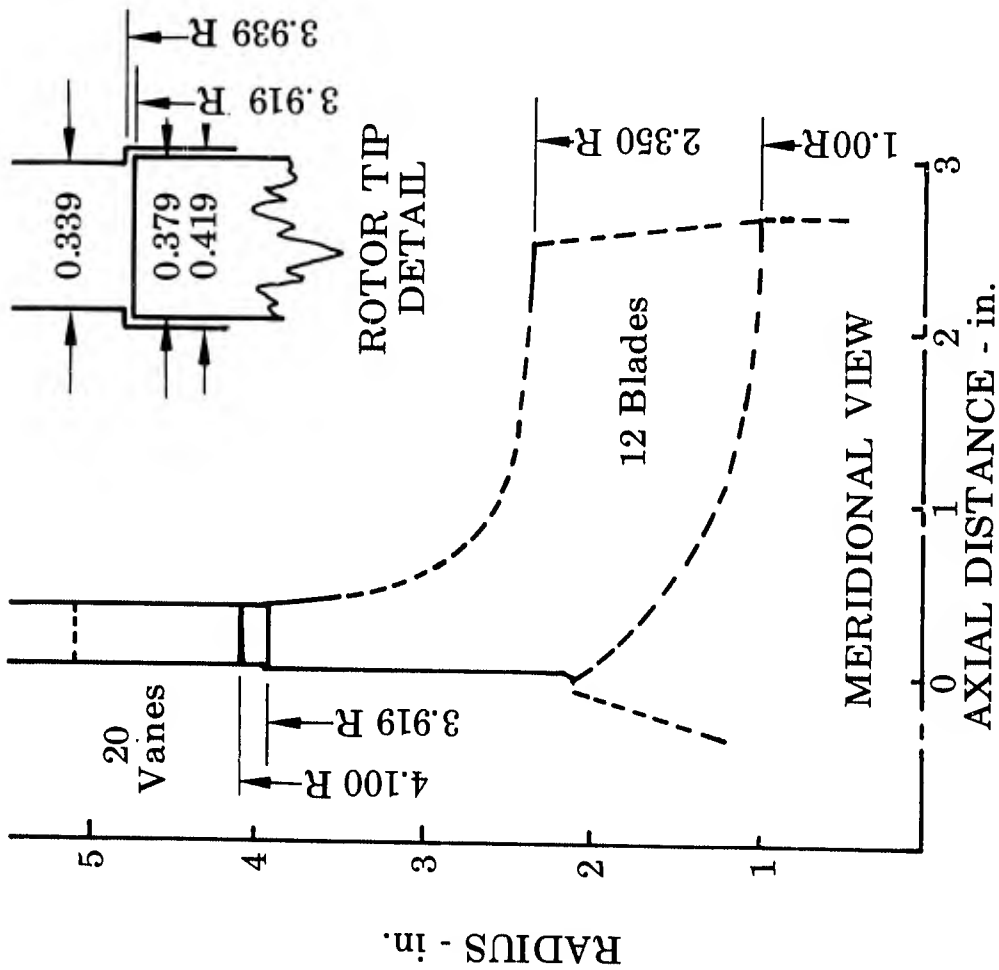


Figure 15. Cooled Turbine Preliminary Design - 75-Degree Nozzle Angle

FD 23259

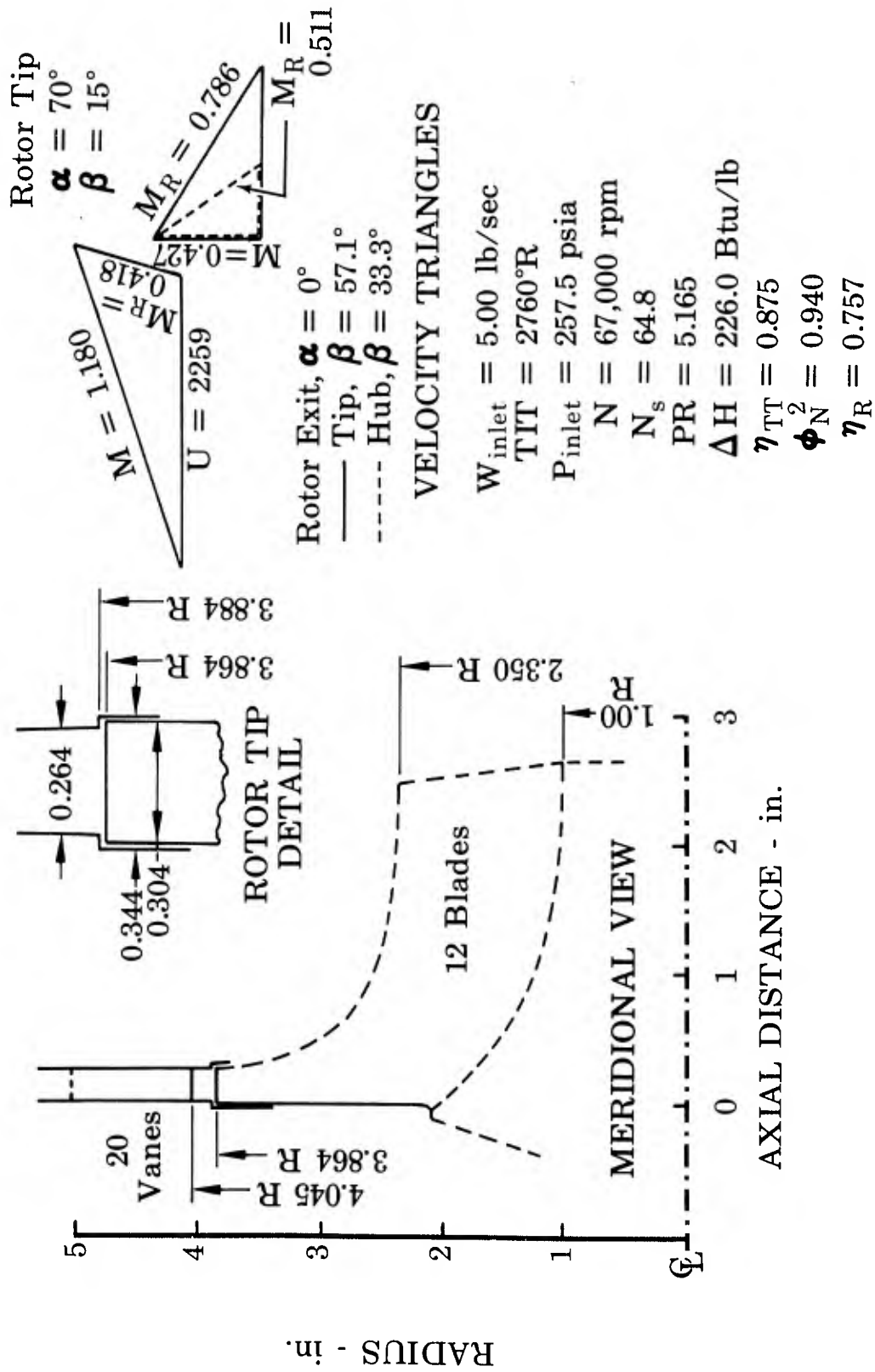
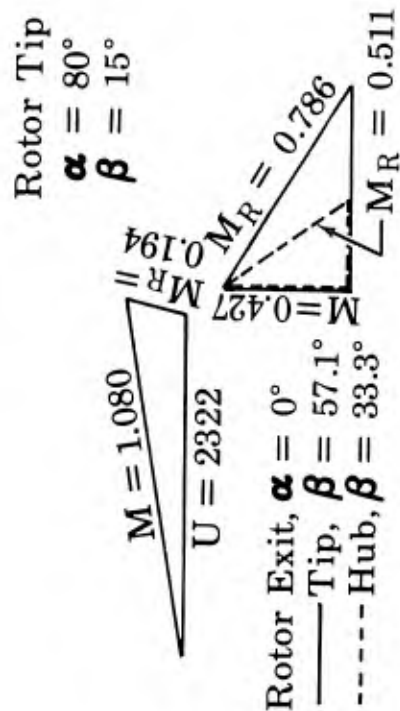


Figure 16. Cooled Turbine Preliminary Design - 70-Degree Nozzle Angle



VELOCITY TRIANGLES

- $W_{inlet} = 5.00$ lb/sec
- TIT = $2760^\circ R$
- $P_{inlet} = 257.5$ psia
- $N = 67,000$ rpm
- $N_s = 64.8$
- PR = 5.165
- $\Delta H = 226.0$ Btu/lb
- $\eta_{TT} = 0.875$
- $\phi_N^2 = 0.940$
- $\eta_R = 0.760$

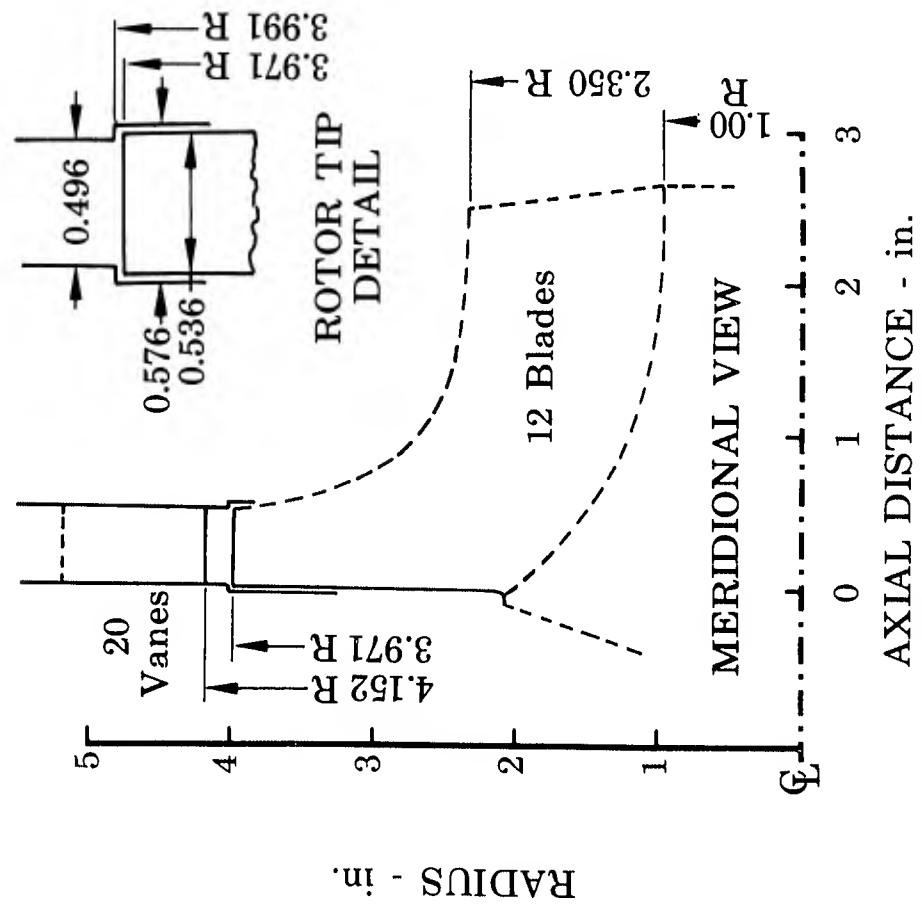


Figure 17. Cooled Turbine Preliminary Design - 80-Degree Nozzle Angle

FD 23261

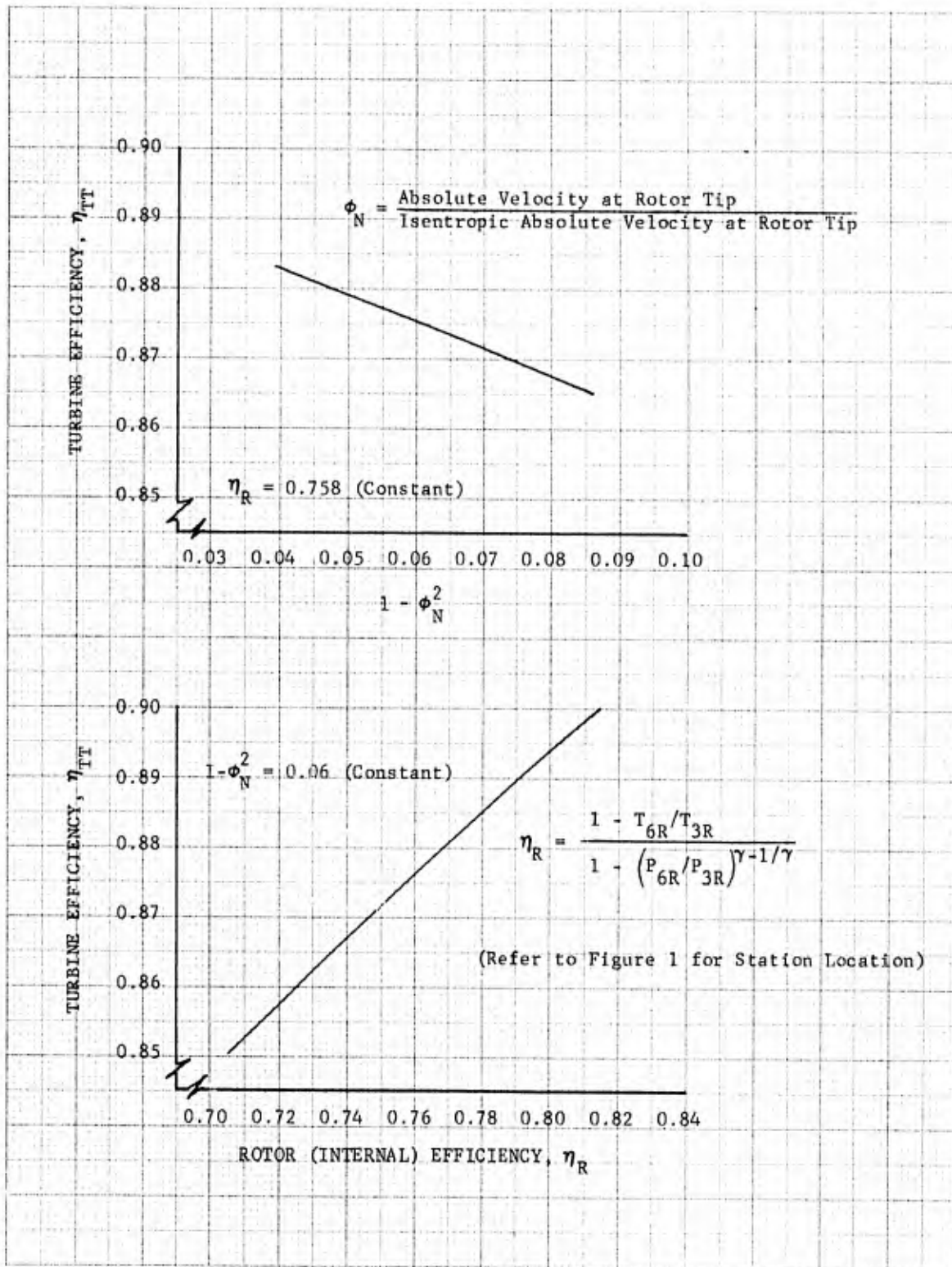


Figure 18. Effects of Nozzle and Rotor Losses on Turbine Efficiency

DF 60054

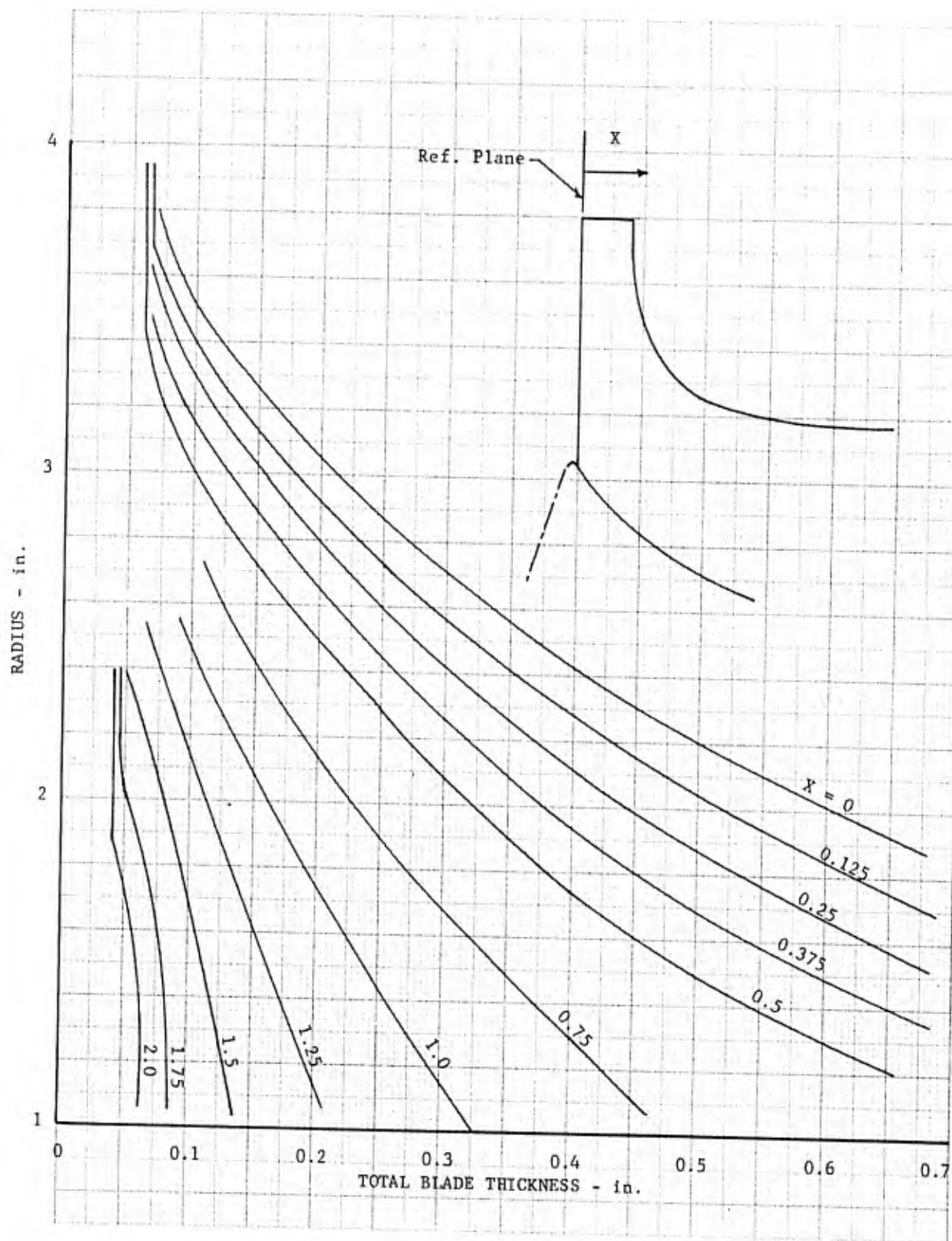


Figure 19. Cooled Turbine Rotor: First-Iteration Blade Thickness Distribution

DF 60053

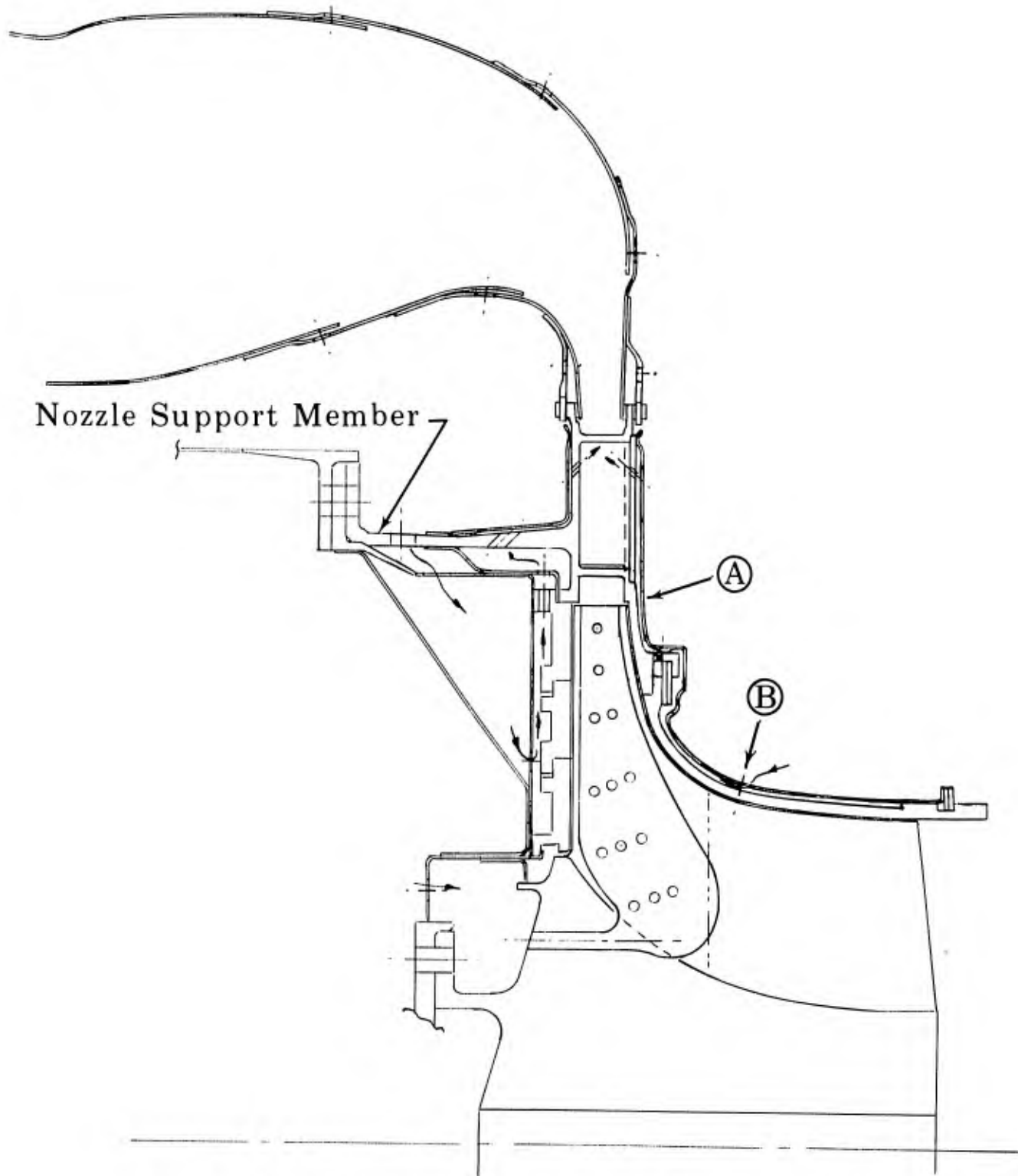


Figure 20. First-Iteration Cooled Turbine Design FD 23262

FD 23263

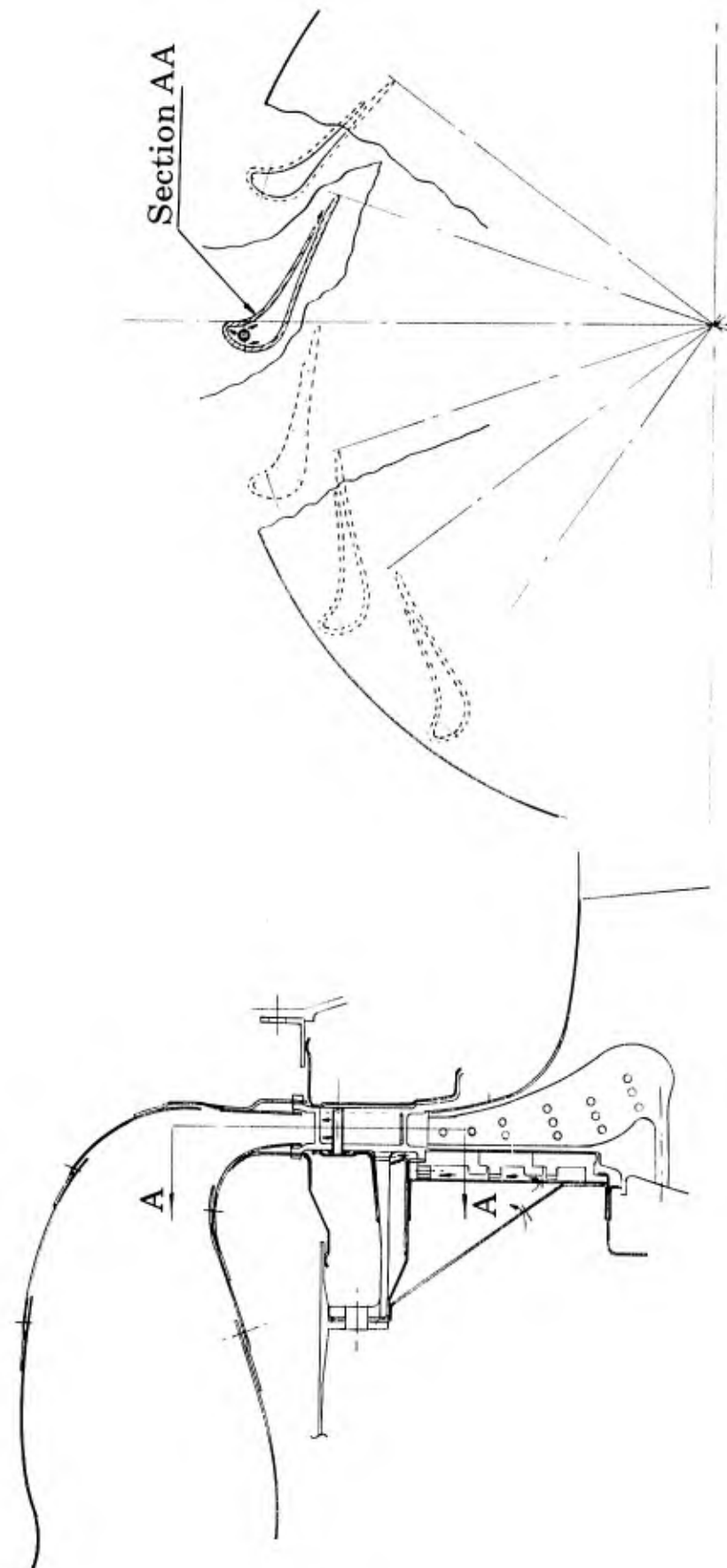


Figure 21. Second-Iteration Cooled Turbine Design

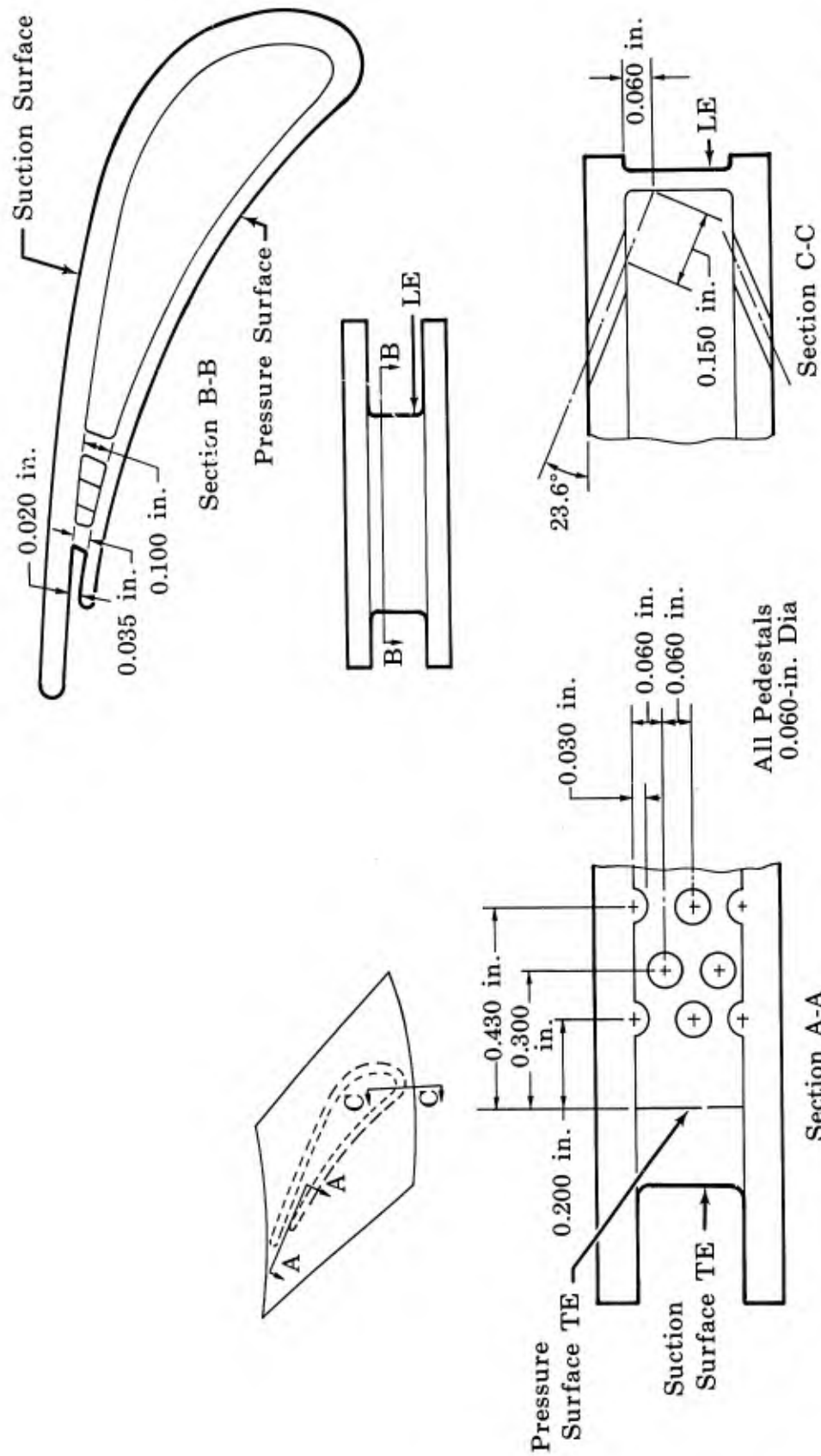


Figure 22. First-Iteration Nozzle Heat Transfer Design

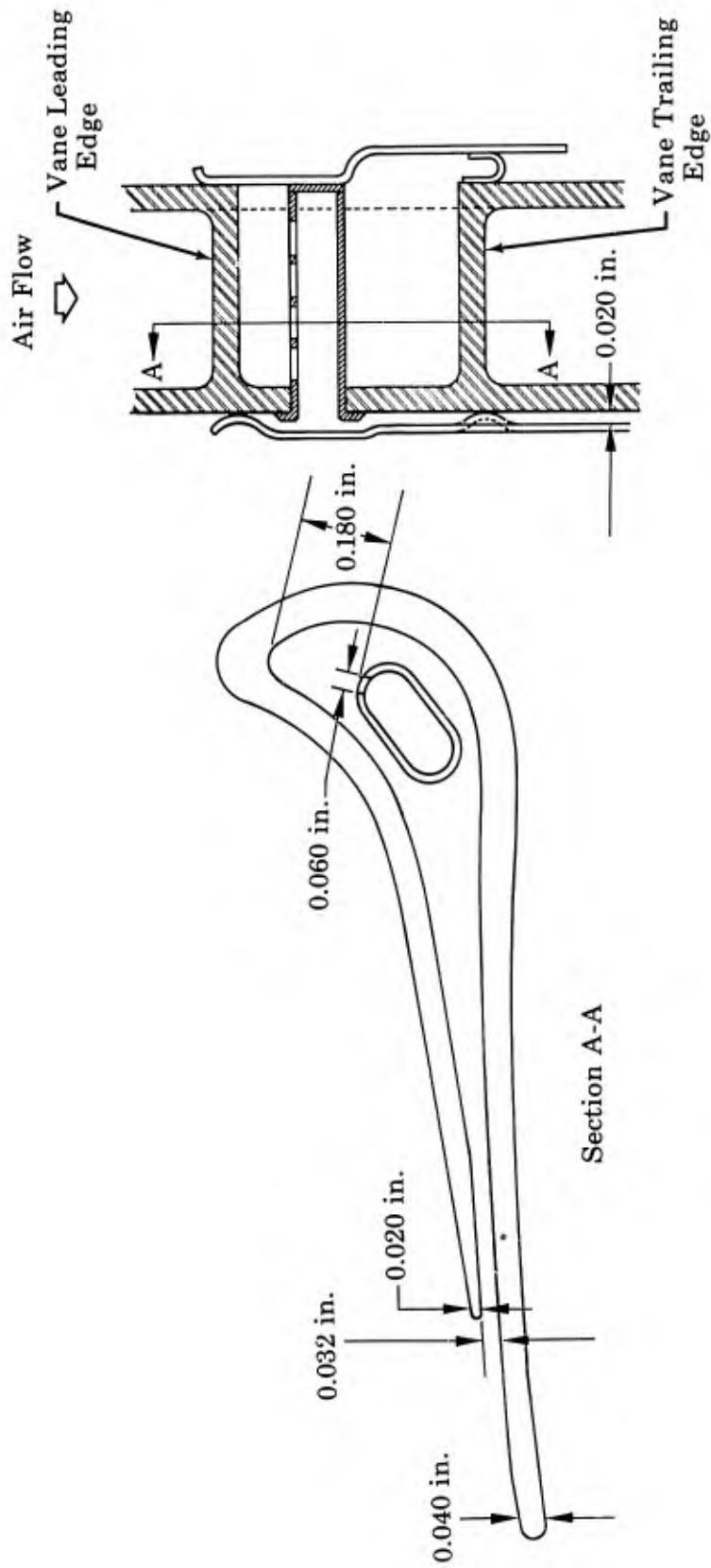


Figure 23. Second-Iteration Nozzle Heat Transfer Design: Nozzle Uses Shroud Air

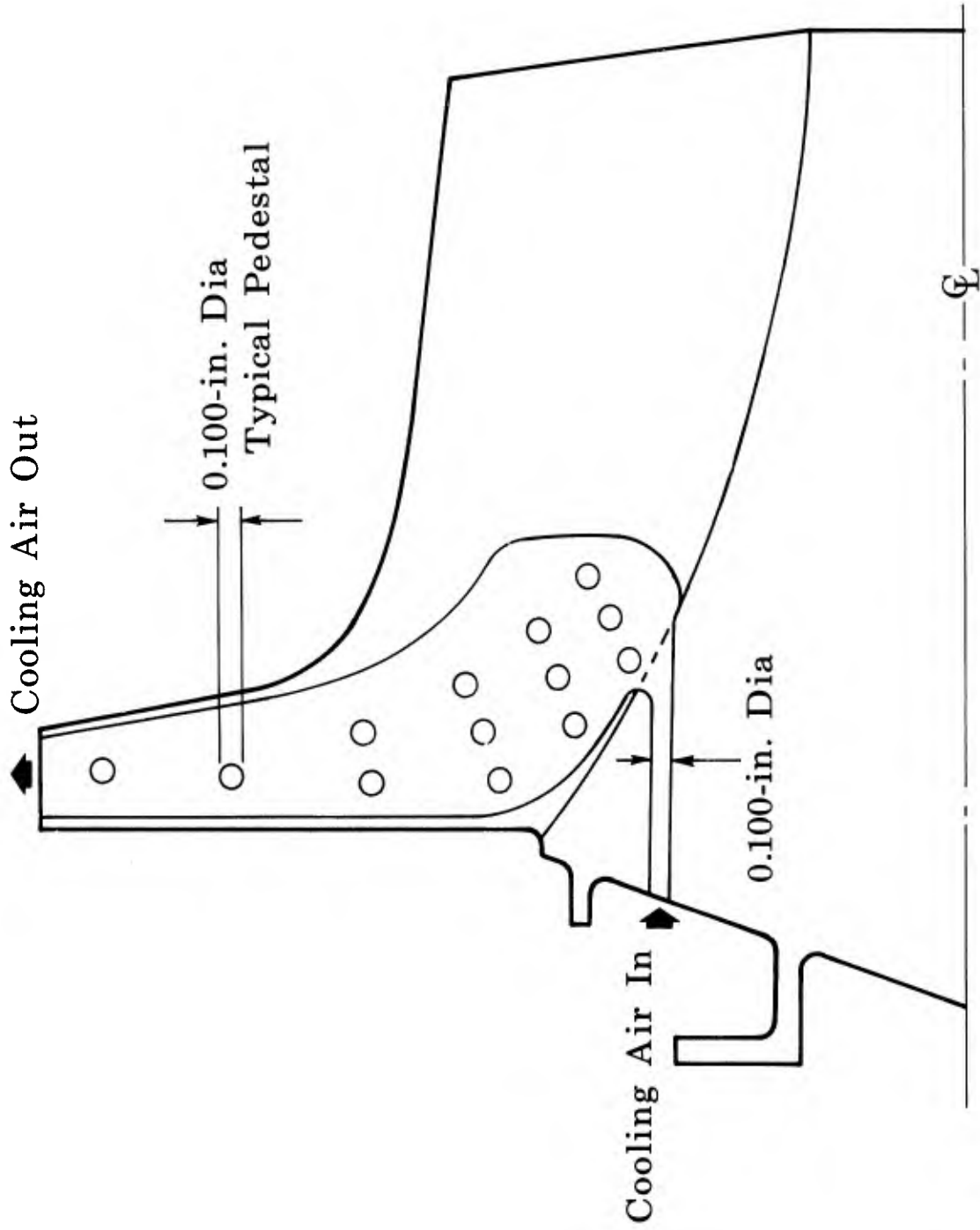


Figure 24. First-Iteration Rotor Heat Transfer Design Shows Reduced Pedestal Density

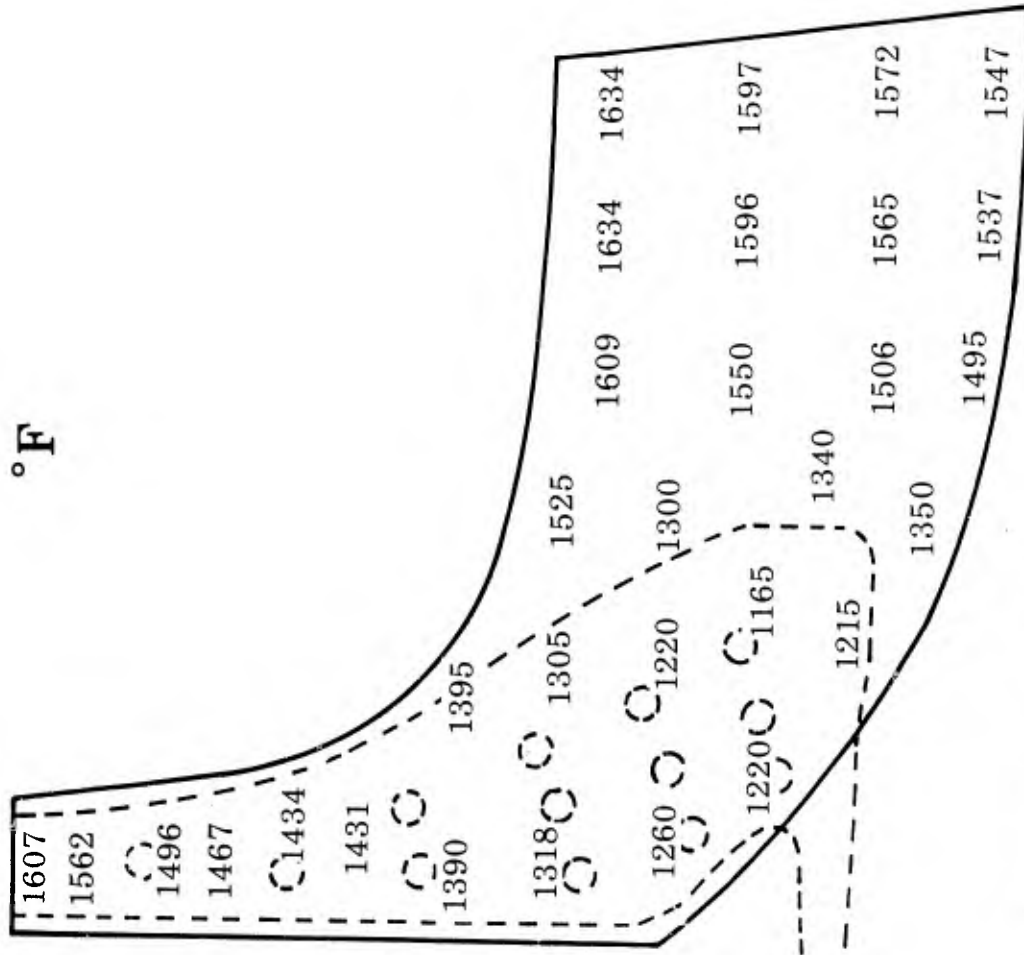


Figure 25. Pressure Surface Temperature Distribution

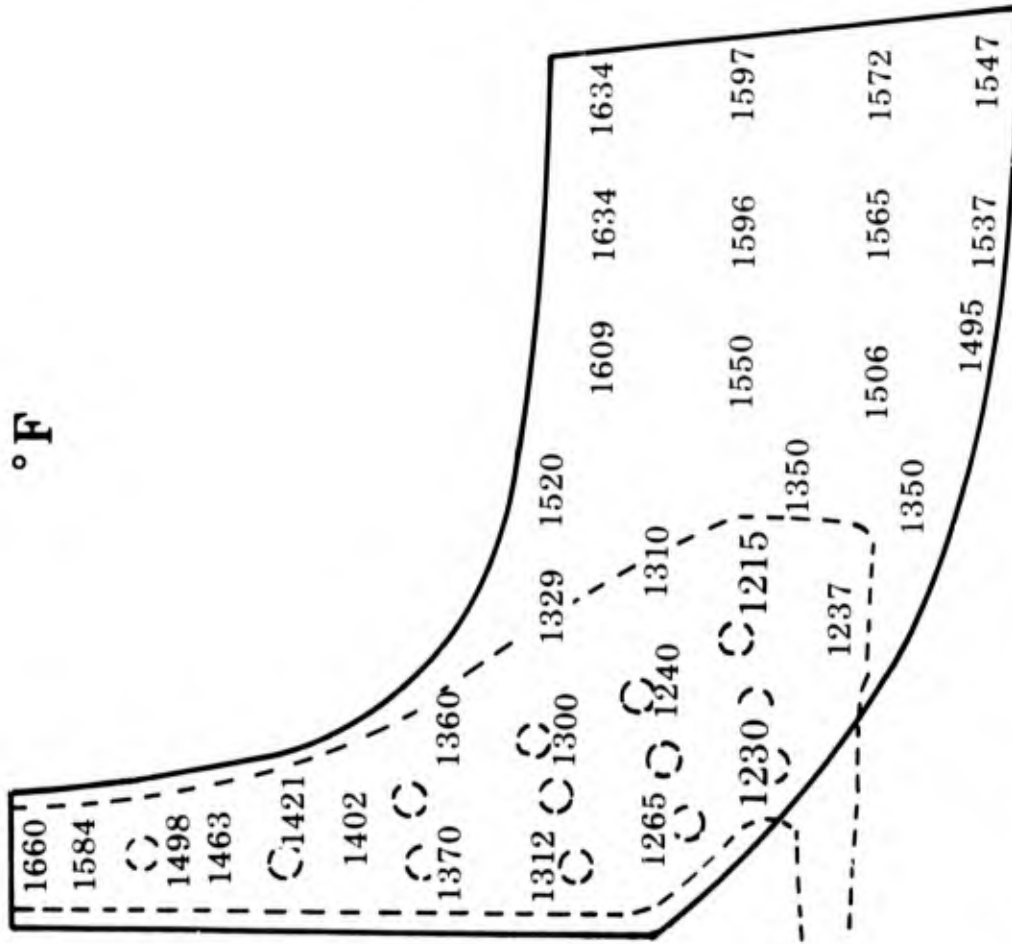


Figure 26. Suction Surface Temperature Distribution

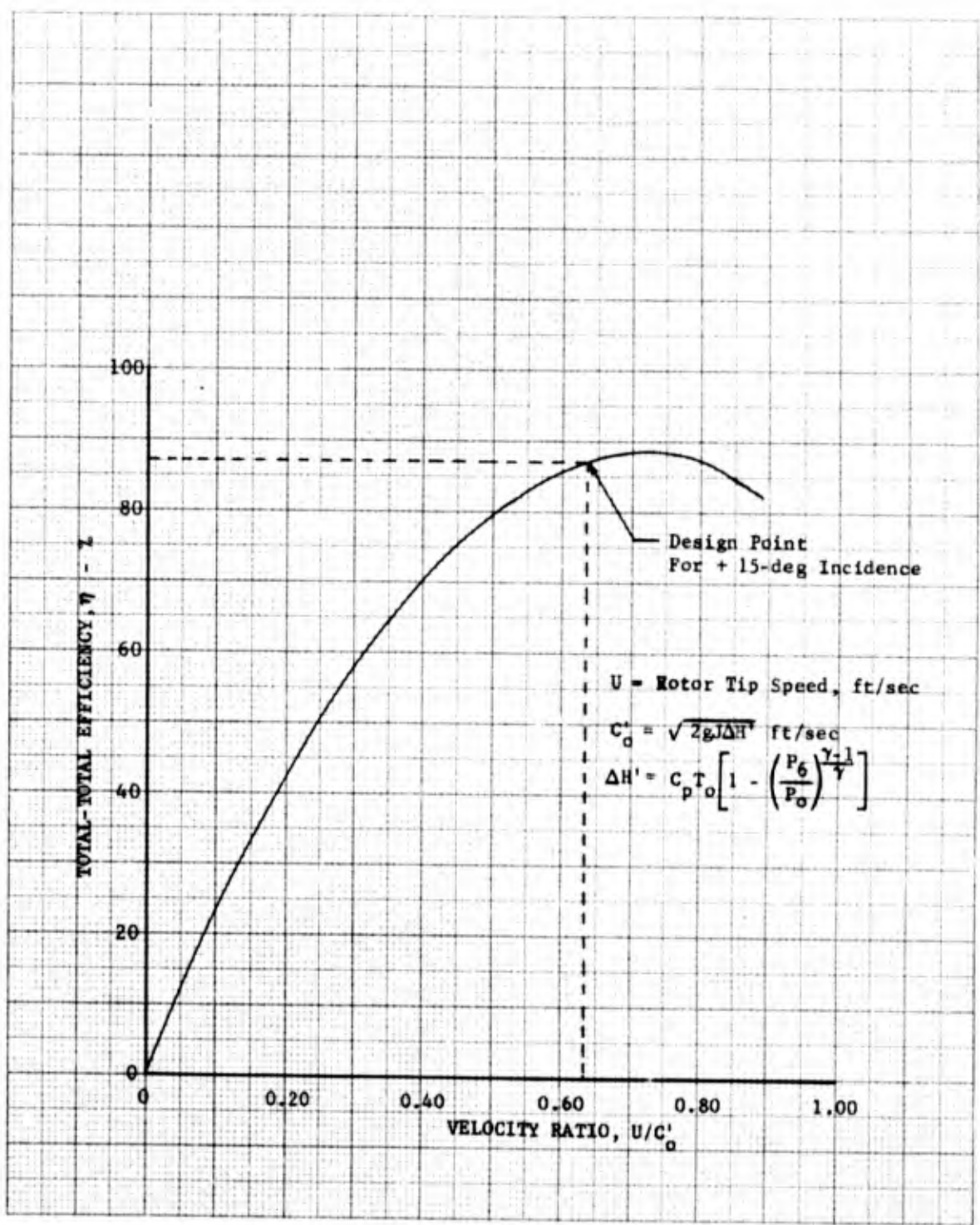


Figure 27. Hot Turbine Part Load Efficiency Estimated From Results of Previous Tests

DF 60052

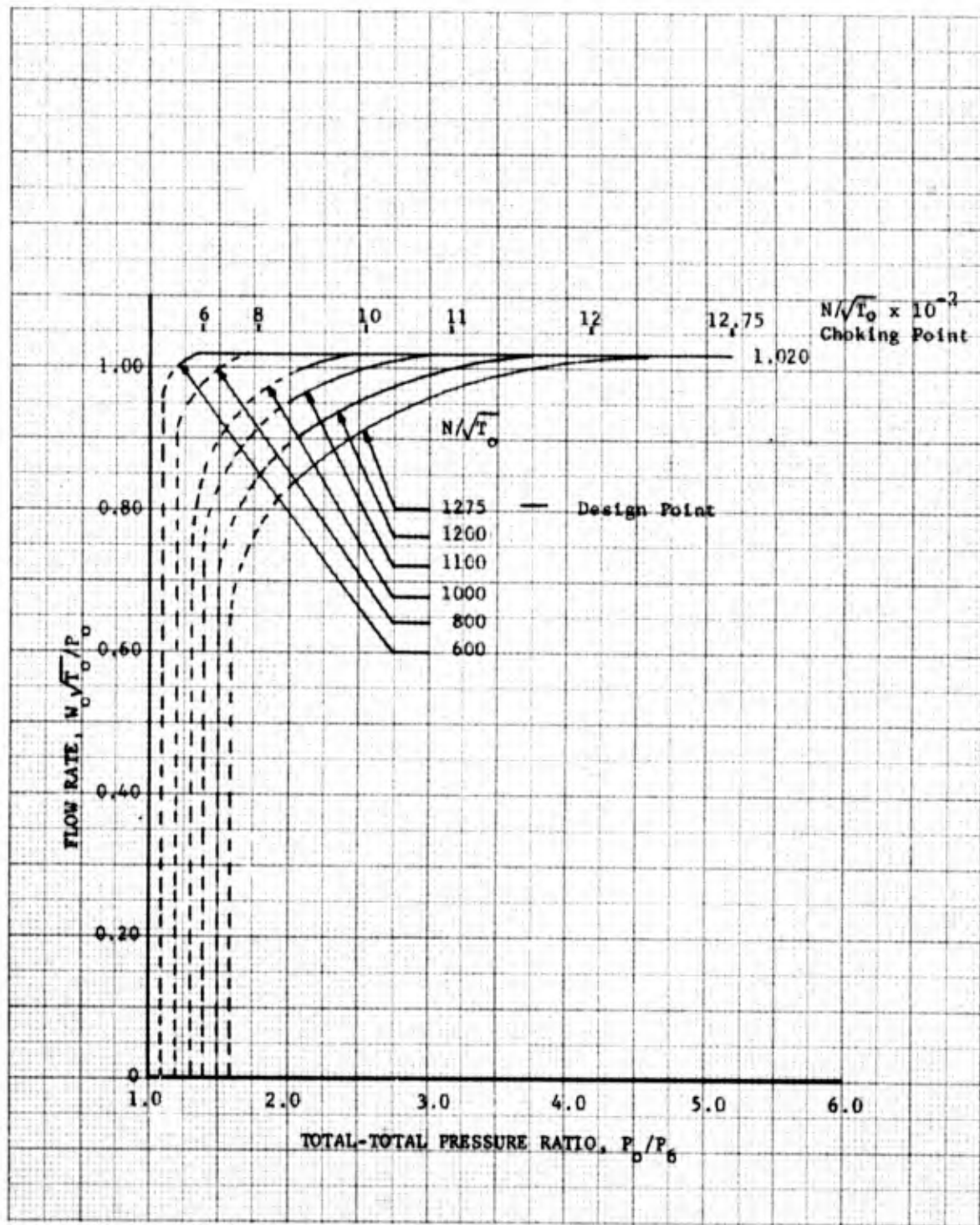


Figure 28. Hot Turbine Swallowing Capacity Estimated From Results of Previous Tests DF 60051